Journal of Sound and Vibration 614 (2025) 119156

Contents lists available at ScienceDirect

Journal of Sound and Vibration

journal homepage: www.elsevier.com/locate/jsvi

Liquid motion in cylindrical containers with elastic covers under external excitation

K. Ren [a], G.X. Wu [b,*]

[a] Department of Civil, Maritime and Environmental Engineering, School of Engineering, University of Southampton, Boldrewood Innovation Campus SO16 7QF, UK
[b] Department of Mechanical Engineering, University College London, Torrington Place, London WC1E 7JE, UK

ARTICLE INFO

Keywords:
Coupled fluid/structure vibration
Transient
Laplace transform
Liquid sloshing
Elastic cover

ABSTRACT

The coupled motion of liquid with an elastic plate or membrane cover in a cylindrical container under external excitation is investigated. Unlike self-oscillation problem at a natural frequency, the problem is fully transient, and it is first converted from the time domain to the *s*-domain through the Laplace transform. For each given *s*, velocity potential for the fluid flow and cover deflection are obtained through the Bessel-Fourier series. The solution in the time domain is then obtained through the inverse Laplace transform with respect to *s*. When doing so analytically, it is necessary to find singularities of the integrand in the entire complex plane *s*. It is shown that these singularities are only on the imaginary axis, corresponding precisely to the natural frequencies of the system and the excitation frequencies. This allows that the final solution to be obtained explicitly, which gives insight how the motion behaves. Extensive results are presented for the time history of the cover deflection and the energy components under various external excitation, including tank motion and external pressure on the cover. The frequency components of the solutions are analysed both at resonance and off-resonance. The energy transfer into the system from external forcings and its redistribution during vibration within the system are analysed.

1. Introduction

The study of sloshing dynamics of liquids in containers has important applications across various fields, such as marine, civil, coastal, building and space engineering. Therefore, research in this area has been undertaken extensively. When the liquid surface in a rigid container is free and the amplitude of the sloshing wave is small compared with the dimension of the container, linear velocity potential theory is commonly used. Various analytical and numerical procedures have been developed to obtain solutions for a variety of container shapes [1–4]. The effect of the viscous fluid has also been examined based on the continuity and linearised Navier-Stokes equations [5], and it has been found that it decreases quickly as the viscosity reduces. When the amplitude of the sloshing wave is not small, velocity potential theory with nonlinear free surface boundary conditions is commonly used. Various numerical methods have been adopted. These include works based on boundary element method [6], finite element method [7,8], and finite difference method [9]. When viscosity does have a major effect, Navier-Stokes equations are then used [10,11]. In addition, extensive experimental work was also conducted [12,13].

When some components of the container are no longer rigid, or there is an elastic cover on the upper surface of the liquid, the

* Corresponding author.
E-mail addresses: k.ren@soton.ac.uk (K. Ren), g.wu@ucl.ac.uk (G.X. Wu).

https://doi.org/10.1016/j.jsv.2025.119156
Received 3 January 2025; Received in revised form 23 April 2025; Accepted 24 April 2025
Available online 1 May 2025

vibration of elastic structures is coupled with the liquid sloshing. The coupled motion may significantly differ from that in a rigid container. Typical works on the two-dimensional problem include free vibration problem in a rectangular tank with rigid side and bottom walls, where the liquid surface is fully covered by an elastic membrane or plate [14], based on a horizontal mode expansion method. Bauer and Eidel [15] extended this analysis to cases where the liquid surface was partly covered by an elastic structure, with one end clamped to the side wall and the other end is free. They investigated the natural frequencies of the coupled system. The liquid motion in the container undergoing the forced motion was also considered by them in the work, but it included only the frequency component at the excitation frequency, and all the natural modes were ignored. Other studies have focused on containers with elastic side walls, with a notable example being that in [16]. In that work, the solution obtained was an approximation, as the pressure of the liquid flow obtained from the Bernoulli equation for the wetted part of the side wall was extended to the dry part. Bauer [17] investigated the natural frequencies of liquid motion with an elastic cover in a vertical circular container, through a Bessel-Fourier series expansion approach. Amabili [18] studied the case where the inner part of the liquid surface was covered by an elastic plate circular plate, while the external part remains free. The Rayleigh-Ritz method was used. Kim and Lee [19] further considered the scenario where a doughnut-shaped plate partially covered the liquid surface in a vertical circular container based on the Rayleigh-Ritz method. Recently, Ren et al. [20] further considered the free vibration problem in a vertical circular cylinder with an elastic plate. Two approaches different from that in [17] were used, based on horizontal mode through Bessel-Fourier series expansion and vertical mode expansion, respectively. Two sets of explicit equations were derived for natural frequencies of the coupling system, and they were found to be identical through the residue theorem. A more recent and relevant study by Shen et al. [21] examined the coupled free motion in a tank equipped with plate baffles, while Kim and Kwak [22] investigated the coupled motion of a circular plate resting on the free surface of liquid in a circular cylindrical container. The analysis for free motion of liquid in a three-dimensional vertical rectangular (or cubic) container with an elastic cover was undertaken by Bauer et al. [23] and Ren et al. [24]. It is worth noting that in [23], the double series expansion used for the elastic plate is valid only for the simply supported edge condition, while in [24] the expansion can be applied to any edge conditions.

Much of the work above has mainly considered self-oscillation caused by some initial disturbance, or oscillation at the excitation frequency only and the motion at the natural modes are ignored. In such a case, the solution is obtained for motion at each individual frequency and the time factor can be taken out. In many practical problems, the container is under persistent excitation, and the excitation may be fully transient. Even when the excitation consists of just periodic components, the sloshing motion will have components not just at all the excitation frequencies but also at the natural frequencies of the tank. All these components are coupled through initial conditions and the time factor cannot be simply taken out. As a result, the problem will be fully time dependent. This makes the problem completely different from that of self-oscillation. In this work, we present an analytical scheme for liquid motion in a vertical circular container with an elastic cover subject to external excitation. The present work is based on assumptions of ideal liquid and small amplitude oscillations. The former ignores the viscosity as its effect is usually small unless the oscillation is over a long time relative to the typical period of the motion (Wu et al. [5]), or the excitation is at one of the natural frequencies. The latter ignores the nonlinear terms in the equations of the cover, as the linear term is dominant at the small amplitude. The forced horizontal motion of the container and external pressure applied on the cover are used as examples and other excitations can be considered similarly. It is also worth mentioning that parametric resonance may occur in reality when a vertical oscillation is present. To model that in the free surface problem, the product term is included and hence modes at sum and difference frequencies occur. To consider this in the case with an elastic cover, some important nonlinear terms in the dynamic and kinematic equations need to be included. However, the focus of the present work is on the motions at the prime frequencies, and therefore, linear theory is used for the cover. In addition, the temporal variation of the external excitation can be arbitrary. The Laplace transform method is used for the transient problem. The velocity potential for the fluid flow is then expanded into Bessel-Fourier series [20] in the horizontal plane and the expansion in the vertical direction is obtained from the Laplace equation. This potential then satisfies all the equations apart from that on the cover. The cover is treated as an elastic plate or membrane and the linear equation of motion is used. The deflection of the cover is also expanded into Bessel-Fourier series. By matching the pressures and the normal velocities of the fluid flow and the cover, the unknown coefficients in both expansions can be obtained. Inverse Laplace transform is then performed to obtain the solution of the problem. This may be straightforward for the free surface problem as its boundary conditions are much simpler and there are no edge conditions. When there is a cover, it becomes less straightforward and there seems little work on the problem. Here this becomes a crucial part of the present work. To perform inverse transform explicitly, all the singularities of the integrand have to be found. As it has to be done in the complex plane, it is usually not a trivial task. In this work we are able to show that singularities are only on the imaginary axis, and they completely match the natural frequencies of the tank, plus those at the excitation frequencies. This makes it possible to perform the inverse Laplace transform explicitly. The result obtained analytically then confirms that the motion has components at all the natural frequencies and at the excitation frequencies. When the excitation frequency is equal to one of natural frequencies, the motion will become larger and larger as time increases, or resonance will occur, as expected. Extensive results are presented for the cover deflection and the energy components of the system, both at resonance and off-resonance over time. For the energy analysis, the results clearly illustrated how the energy transfer from external forcing to the system and its transition among different components during vibration.

The work is organised as follows. The mathematical model and formulations are introduced in Section 2, followed by the energy analysis in Section 3 and results and analysis in Section 4. Conclusions are presented in Section 5.

2. Mathematical model and formulations

2.1. Mathematical modelling

We consider liquid sloshing in a circular cylindrical tank due to some external excitation, as shown in Fig. 1. The tank wall is assumed to be rigid, while an elastic cover, which may be a plate or a membrane, is placed on the top of the liquid surface, where there is an external pressure. Cartesian and cylindrical coordinate systems, O-xyz and O-$r\theta z$, are established. Their origins are both located on the mean upper surface of the liquid, and z-axes point vertically upwards along the mean position of the centre line of the tank. The liquid is assumed to be inviscid and incompressible, and its motion is irrotational. Therefore, the velocity potential Φ can be adopted to describe the motion of the liquid domain, which satisfies the Laplace equation as

$$\nabla^2\Phi + \frac{\partial^2\Phi}{\partial z^2} = \frac{\partial^2\Phi}{\partial x^2} + \frac{\partial^2\Phi}{\partial y^2} + \frac{\partial^2\Phi}{\partial z^2} = \frac{\partial^2\Phi}{\partial r^2} + \frac{1}{r}\frac{\partial\Phi}{\partial r} + \frac{1}{r^2}\frac{\partial^2\Phi}{\partial\theta^2} + \frac{\partial^2\Phi}{\partial z^2} = 0, \tag{1}$$

where ∇^2 refers to the two-dimensional Laplacian.

When the motion amplitude is small compared with the tank dimensions, the boundary conditions may be linearised. In such a case, the deflection W of the elastic cover and the velocity potential satisfy the dynamic condition on $z = 0$ as follows: for a plate,

$$m_e\frac{\partial^2 W}{\partial t^2} + L\nabla^4 W = -\rho\Phi_t - \rho g W + P, \tag{2a}$$

and for a membrane,

$$m_e\frac{\partial^2 W}{\partial t^2} - T\nabla^2 W = -\rho\Phi_t - \rho g W + P. \tag{2b}$$

Specifically, the governing equation for the plate cover involves a biharmonic term $L\nabla^4 W$, and it resists deformation primarily through bending. The governing equation for the membrane involves a term $-T\nabla^2 W$, and it resists deformation mainly through the tension in the membrane. The transversal or in-plane displacements can typically be neglected when the plate is thin and undergoes small deflections, following the works such as Timoshenko and Woinowsky-Krieger [25].

In both cases, the impermeable kinematic condition on $z = 0$ yields

$$\frac{\partial W}{\partial t} = \frac{\partial\Phi}{\partial z}. \tag{3}$$

In (2), L, T and m_e are the flexural rigidity, the membrane tension, and the mass per unit area of the elastic cover, respectively. ρ is the density of the liquid and g is the acceleration due to gravity. $P(x, y, t)$ is an arbitrary external pressure, which can be both spatial and temporal dependent.

Without loss of generality, we may assume that the tank undergoes horizontal oscillation in the direction of $\theta = 0$ with velocity $U(t)$, as motion in any other directions can be considered similarly by redefining θ. The impermeable surface condition on the tank wall can then be expressed as

$$\left.\frac{\partial\Phi}{\partial r}\right|_{r=r_0} = U(t)\cos\theta. \tag{4}$$

On the tank bottom, we have

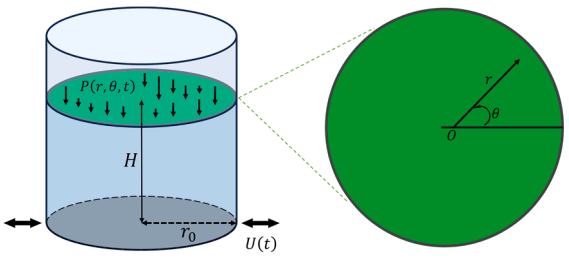

Fig. 1. Sketch of the problem.

$$\left.\frac{\partial\Phi}{\partial z}\right|_{z=-H}=0. \tag{5}$$

In Eqs. (4) and (5), r_0 is the radius of the tank and H is the depth of the liquid. The cover is assumed to extend to the tank wall. For a plate cover, we may consider three types of commonly used edge conditions (Timoshenko & Woinowsky-Krieger [25]), or for clamped edge:

$$W|_{r=r_0}=0,\ \left.\frac{\partial W}{\partial r}\right|_{r=r_0}=0, \tag{6ab}$$

for free edge:

$$\nabla^2 W|_{r=r_0}=\frac{1-\nu}{r_0}\left[\left(\frac{1}{r_0}\frac{\partial^2}{\partial\theta^2}+\frac{\partial}{\partial r}\right)W\right]_{r=r_0}, \tag{7a}$$

$$\left[\frac{\partial}{\partial r}\nabla^2 W\right]_{r=r_0}=-\frac{1-\nu}{r_0^2}\left[\left(\frac{\partial^3}{\partial\theta^2\partial r}-\frac{1}{r_0}\frac{\partial^2}{\partial\theta^2}\right)W\right]_{r=r_0}, \tag{7b}$$

and for simply supported edge:

$$W|_{r=r_0}=0,\ \nabla^2 W|_{r=r_0}=\frac{1-\nu}{r_0}\left[\left(\frac{1}{r_0}\frac{\partial^2}{\partial\theta^2}+\frac{\partial}{\partial r}\right)W\right]_{r=r_0}. \tag{8ab}$$

For a membrane cover, the edge condition may be assumed as that in Eq. (6a).

The initial conditions may be obtained from the dynamic and kinematic boundary conditions, or (2) and (3). Assuming that there is no motion when $t<0$. Integrating (2) from $t=0^-$ to $t=0^+$, and assuming that there is no impulse, we have

$$\Phi|_{z=0}=-\frac{m_e}{\rho}W_t=-\frac{m_e}{\rho}\left.\frac{\partial\Phi}{\partial z}\right|_{z=0},\ t=0^+. \tag{9}$$

The other initial condition can be written as

$$W=0,\ t=0. \tag{10}$$

2.2. Laplace transform method for the transient motion analysis

Laplace transform $\mathfrak{L}$ is applied to investigate the liquid sloshing due to the forced motion of the container and the external pressure on the elastic cover. Applying $\mathfrak{L}$ to Eqs. (2a) for an elastic plate and (3), denoting $\mathscr{W}(s)=\mathfrak{L}\{W(t)\}$, $\mathscr{F}(s)=\mathfrak{L}\{\Phi(t)\}$ and $\mathscr{P}(s)=\mathfrak{L}[P(t)]$ together with initial conditions in (9) and (10), we have

$$L\nabla^4\mathscr{W}(s)+\left(m_e s^2+\rho g\right)\mathscr{W}(s)=-\rho s\mathscr{F}(s)|_{z=0}+\mathscr{P}(s), \tag{11}$$

$$s\mathscr{W}(s)=\mathscr{F}_z(s)|_{z=0}. \tag{12}$$

Similarly, $\mathfrak{L}$ is also performed on the other boundary conditions, which yields

$$\frac{\partial\mathscr{F}(s)}{\partial r}=\mathscr{U}(s)\cos\theta, \tag{13a}$$

and

$$\left.\frac{\partial\mathscr{F}(s)}{\partial z}\right|_{z=-H}=0, \tag{13b}$$

where $\mathscr{U}(s)=\mathfrak{L}\{U(t)\}$.

As $P(r,\theta,t)$ can be arbitrarily chosen, without loss of generality, we can write

$$P(r,\theta,t)=\sum_{n=0}^{\infty}P_n(r,t)\cos n\theta, \tag{14}$$

where $P_n(r,t)$ are prescribed. The functions $\mathscr{T}(r,\theta,s)$ and $\mathscr{W}(r,\theta,s)$ can be expanded into the following Bessel-Fourier series [20]

$$\mathscr{T}(r,\theta,z,s) = \mathscr{U}(s)\ r\cos\theta + \sum_{n=0}^{\infty}\sum_{m=1}^{\infty} J_n(\alpha_{nm}r)\ \mathscr{A}_{nm}(s)\cos n\theta \frac{\cosh\alpha_{nm}(z+H)}{\cosh\alpha_{nm}H}, \tag{15}$$

while $\mathscr{W}(r,\theta,s)$ is first expanded into Fourier series

$$\mathscr{W}(r,\theta,s) = \sum_{n=0}^{\infty} \mathscr{W}_n(r,s)\cos n\theta, \tag{16}$$

where $\alpha_{nm}r_0$ are the zeros of the first-order derivative of Bessel function, or $J_n'(\alpha_{nm}r_0) = 0$.

Due to the orthogonality of trigonometric functions, Eqs. (11) and (12) can be written in terms of $\mathscr{W}_n$ as

$$L\left(\frac{\partial^2}{\partial r^2} + \frac{1}{r}\frac{\partial}{\partial r} - \frac{n^2}{r^2}\right)^2 \mathscr{W}_n(r,s) + \left(m_e s^2 + \rho g\right)\ \mathscr{W}_n(r,s) = -\sum_{m=1}^{\infty} \rho s \mathscr{A}_{nm}(s) J_n(\alpha_{nm}r) - \rho s\,\mathscr{U}(s)\ r\delta_{n1} + \mathscr{P}_n(r,s), \tag{17}$$

and

$$s\,\mathscr{W}_n(r,s) = \sum_{m=1}^{\infty} \alpha_{nm}\tanh\alpha_{nm}H\ J_n(\alpha_{nm}r)\ \mathscr{A}_{nm}(s). \tag{18}$$

We further expand $\mathscr{W}_n$ as

$$\mathscr{W}_n(r,s) = \sum_{m=1}^{\infty} e_{nm}(s)\ J_n(\alpha_{nm}r). \tag{19}$$

Multiplying both sides of Eq. (17) by $rJ_n(\alpha_{nm}r)$, using the orthogonality of the Bessel functions, following the procedure leading to Eqs. (28) and (29) in [20], Eqs. (17) and (18) can lead to the equations below

$$\frac{LK_m}{\Omega_{nm}} + \left(m_e s^2 + \rho g\right)e_{nm}(s) + \rho s \mathscr{A}_{nm}(s) = \frac{\mathscr{H}_{nm}}{\Omega_{nm}} - \frac{\rho s\,\mathscr{U}(s)\delta_{n1}}{\Omega_{nm}} \times \frac{r_0^2\ J_2(\alpha_{1m}r_0)}{\alpha_{1m}}, \tag{20}$$

and

$$\mathscr{A}_{nm}(s) = \frac{s e_{nm}(s)}{\alpha_{nm}\tanh\alpha_{nm}H}, \tag{21}$$

where

$$\mathscr{H}_{nm}(s) = \int_0^{r_0} \mathscr{P}_n(r,s) r J_n(\alpha_{nm}r)\mathrm{d}r, \tag{22}$$

$$\Omega_{nm} = \frac{\left(\alpha_{nm}^2 r_0^2 - n^2\right)J_n^2(\alpha_{nm}r_0)}{2\alpha_{nm}^2}, \tag{23}$$

$$K_m = r_0 J_n(\alpha_{nm}r_0)\frac{\partial \mathscr{L}_n}{\partial r}\bigg|_{r=r_0} - r_0\alpha_{nm}^2 J_n(\alpha_{nm}r_0)\frac{\partial \mathscr{W}_n}{\partial r}\bigg|_{r=r_0} + \alpha_{nm}^4 e_{nm}\Omega_{nm}, \tag{24}$$

and $\frac{\partial \mathscr{L}_n}{\partial r}|_{r=r_0} = \left[\left(\frac{\partial^2}{\partial r^2} + \frac{1}{r}\frac{\partial}{\partial r} - \frac{n^2}{r^2}\right)\frac{\partial \mathscr{W}_n}{\partial r}\right]_{r=r_0}$ and $\frac{\partial \mathscr{W}_n}{\partial r}|_{r=r_0}$ are two unknowns to be determined by the edge conditions. Here it is important to note that the derivatives of $\mathscr{W}_n$ in Eq. (17) is treated by integration by parts first and (19) is used only for $\mathscr{W}_n$ but not its derivatives directly. The reason for this is similar to that in Eq. (2.11) of Ren *et al* [26].

Using (21) to eliminate $\mathscr{A}_{nm}(s)$ in (20), we have

$$Lr_0\left(\frac{\partial \mathscr{L}_n}{\partial r}\bigg|_{r=r_0} - \alpha_{nm}^2\frac{\partial \mathscr{W}_n}{\partial r}\bigg|_{r=r_0}\right)J_n(\alpha_{nm}r_0) + \left[L\alpha_{nm}^4 + \rho g + m_e s^2 + \frac{\rho s^2}{\alpha_{nm}\tanh\alpha_{nm}H}\right]\Omega_{nm}e_{nm}(s) = \mathscr{H}_{nm}(s) - \frac{\rho s\,\mathscr{U}(s) r_0^2 J_2(\alpha_{1m}r_0)\delta_{n1}}{\alpha_{1m}}, \tag{25}$$

which gives

$$e_{nm}(s) = \frac{\left\{ \mathscr{H}_{nm}(s) - \frac{\rho s \mathscr{U}(s)\ r_0^2 J_2(\alpha_{1m} r_0)\delta_{n1}}{\alpha_{1m}} - L r_0 J_n(\alpha_{nm} r_0) \left(\left.\frac{\partial \mathscr{L}_n}{\partial r}\right|_{r=r_0} - \alpha_{nm}^2 \left.\frac{\partial \mathscr{W}_n}{\partial r}\right|_{r=r_0} \right) \right\}}{\mathscr{K}(s, \alpha_{nm})\ \Omega_{nm}}, \tag{26}$$

where

$$\mathscr{K}(s, \alpha_{nm}) = L\alpha_{nm}^4 + \rho g + s^2 \left(m_e + \frac{\rho}{\alpha_{nm} \tanh \alpha_{nm} H} \right). \tag{27}$$

By applying the Laplace transform to the edge conditions and further using the expansion from Eq. (19), we obtain the following clamped edge conditions

$$\left.\frac{\partial \mathscr{W}_n}{\partial r}\right|_{r=r_0} = 0, \quad \mathscr{W}_n(r = r_0) = 0. \tag{28a,b}$$

From (28*b*), we have

$$\left.\frac{\partial \mathscr{L}_n}{\partial r}\right|_{r=r_0} = \frac{Y_n}{Z_n}, \tag{29}$$

where $Y_n = Y_n^{(\mathscr{U})} + Y_n^{(\mathscr{P})}$,

$$Y_n^{(\mathscr{U})}(s) = -\frac{\rho s r_0\, \mathscr{U}(s)\delta_{n1}}{L} \sum_{m^*=1}^{\infty} \frac{J_2(\alpha_{1m^*} r_0) J_1(\alpha_{1m^*} r_0)}{\mathscr{K}(s, \alpha_{1m^*})\ \Omega_{1m^*} \alpha_{1m^*}} = -\frac{\rho s\, \mathscr{U}(s)\delta_{n1}}{L} \sum_{m^*=1}^{\infty} \frac{J_1^2(\alpha_{1m^*} r_0)}{\mathscr{K}(s, \alpha_{1m^*})\ \Omega_{1m^*} \alpha_{1m^*}^2}, \tag{30a}$$

$$Y_n^{(\mathscr{P})}(s) = \frac{1}{L r_0} \sum_{m^*=1}^{\infty} \frac{\mathscr{H}_{nm^*}(s) J_n(\alpha_{nm^*} r_0)}{\mathscr{K}(s, \alpha_{nm^*})\ \Omega_{nm^*}}, \tag{30b}$$

due to $\mathscr{U}(s)$ and $\mathscr{P}(s)$, respectively, and

$$Z_n(s) = \sum_{m^*=1}^{\infty} \frac{J_n^2(\alpha_{nm^*} r_0)}{\Omega_{nm^*} \mathscr{K}(s, \alpha_{nm^*})}. \tag{31}$$

In (30*a*), the recurrence relation of Bessel functions (Eq. (9.1.27) in Abramowitz & Stegun [27]), together with $J_1'(\alpha_{1m^*} r_0) = 0$ has been used.

Therefore, from (19), we have

$$\mathscr{W}_n(r, s) = \frac{1}{Z_n} \sum_{m=1}^{\infty} \frac{J_n(\alpha_{nm} r)}{\mathscr{K}(s, \alpha_{nm})\ \Omega_{nm}} \left(X_{nm}^{(\mathscr{P})}(s) - \frac{\rho s r_0\, \mathscr{U}(s)\delta_{n1} J_1(\alpha_{1m} r_0)}{\alpha_{1m}^2} X_m^{(\mathscr{U})}(s) \right), \tag{32}$$

where

$$X_{nm}^{(\mathscr{P})}(s) = \sum_{m^*=1}^{\infty} \frac{J_n(\alpha_{nm^*} r_0)}{\Omega_{nm^*} \mathscr{K}(s, \alpha_{nm^*})} [\mathscr{H}_{nm}(s) J_n(\alpha_{nm^*} r_0) - \mathscr{H}_{nm^*}(s) J_n(\alpha_{nm} r_0)], \tag{33}$$

and

$$X_m^{(\mathscr{U})}(s) = \sum_{m^*=1}^{\infty} \frac{J_1^2(\alpha_{1m^*} r_0)}{\mathscr{K}(s, \alpha_{1m^*})\ \Omega_{1m^*}} \left(1 - \frac{\alpha_{1m}^2}{\alpha_{1m^*}^2} \right). \tag{34}$$

Before we perform the inverse Laplace transform to (32), attention may be needed when $\mathscr{K}(s, \alpha_{nm})$ tends to zero. Assume that it happens when $m = m'$, or

$$\Delta_n = \mathscr{K}(s, \alpha_{nm'}) \to 0. \tag{35}$$

In such a case, the corresponding term $\mathscr{K}(s, \alpha_{nm^*})$ in $X_{nm}^{(\mathscr{P})}$, $X_m^{(\mathscr{U})}$ and Z_n also tend to zero at $m^* = m'$. Therefore, we have

$$\mathscr{W}_n(r,s) = \lim_{\Delta_n\to 0}\frac{1}{Z_n\Delta_n}\sum_{m=1}^{\infty}\frac{\Delta_n X_{nm}^{(\mathscr{P})}\,J_n(\alpha_{nm}r)}{\Omega_{nm}\mathscr{K}(s,\alpha_{nm})} - \delta_{n1}\lim_{\Delta_1\to 0}\frac{\rho s r_0\,\mathscr{U}(s)}{Z_1\Delta_1}\sum_{m=1}^{\infty}\frac{\Delta_1 X_m^{(\mathscr{U})}\,J_1(\alpha_{1m}r_0)\,J_1(\alpha_{1m}r)}{\mathscr{K}(s,\alpha_{1m})\,\alpha_{1m}^2\,\Omega_{1m}}$$

$$= \frac{X_{nm'}^{(\mathscr{P})}(s)J_n(\alpha_{nm'}r)}{J_n^2(\alpha_{nm'}r_0)} + \sum_{m=1,m\neq m'}^{\infty}\frac{J_n(\alpha_{nm}r)\,[\mathscr{H}_{nm}(s)J_n(\alpha_{nm'}r_0) - \mathscr{H}_{nm'}(s)J_n(\alpha_{nm}r_0)]}{\Omega_{nm}J_n(\alpha_{nm'}r_0)\mathscr{K}(s,\alpha_{nm})} \tag{36}$$

$$-\delta_{n1}\rho s r_0\,\mathscr{U}(s)\left[\frac{X_{m'}^{(\mathscr{U})}}{\alpha_{1m'}^2}\frac{J_1(\alpha_{1m'}r)}{J_1(\alpha_{1m'}r_0)} + \sum_{m=1,m\neq m'}^{\infty}\frac{J_1(\alpha_{1m}r_0)\,J_1(\alpha_{1m}r)}{\mathscr{K}(s,\alpha_{1m})\,\alpha_{1m}^2\,\Omega_{1m}}\left(1-\frac{\alpha_{1m}^2}{\alpha_{1m'}^2}\right)\right],$$

which is finite. Here, the Δ_n term at $m^* = m'$ in $X_{m'}^{(\mathscr{U})}$ and $X_{nm'}^{(\mathscr{P})}$ will not cause problem because $1-\alpha_{1m'}^2/\alpha_{1m^*}^2 = 0$, and $\mathscr{H}_{nm'}(s)J_n(\alpha_{nm^*}r_0) - \mathscr{H}_{nm^*}(s)J_n(\alpha_{nm'}r_0) = 0$.

From (16) and (32), we have

$$\mathscr{W}(r,\theta,s) = \sum_{n=0}^{\infty}\mathscr{W}_n(r,s)\cos n\theta = \sum_{n=0}^{\infty}\left[\frac{1}{Z_n}\sum_{m=1}^{\infty}\frac{J_n(\alpha_{nm}r)X_{nm}^{(\mathscr{P})}}{\mathscr{K}(s,\alpha_{nm})\,\Omega_{nm}}\right]\cos n\theta + \mathscr{U}(s)\mathscr{X}(r,s)\cos\theta, \tag{37}$$

where

$$\mathscr{X}(r,s) = -\frac{\rho s r_0}{Z_1}\sum_{m=1}^{\infty}\frac{J_1(\alpha_{1m}r)\,J_1(\alpha_{1m}r_0)\,X_m^{(\mathscr{U})}}{\mathscr{K}(s,\alpha_{1m})\,\alpha_{1m}^2\Omega_{1m}}. \tag{38}$$

The deflection of the plate $W(r,\theta,t)$ can be obtained by performing the inverse Laplace transform $\mathfrak{L}^{-1}$ to $\mathscr{W}(r,\theta,s)$, as

$$W(r,\theta,t) = \mathfrak{L}^{-1}[\mathscr{W}(r,\theta,s)] = \cos\theta\times\mathfrak{L}^{-1}[\mathscr{U}(s)\mathscr{X}(r,s)] + \sum_{n=0}^{\infty}\cos n\theta\times\mathfrak{L}^{-1}\left[\frac{1}{Z_n}\sum_{m=1}^{\infty}\frac{J_n(\alpha_{nm}r)X_{nm}^{(\mathscr{P})}}{\mathscr{K}(s,\alpha_{nm})\,\Omega_{nm}}\right]. \tag{39}$$

For the term related to $\mathscr{U}(s)$, we may first consider

$$\mathfrak{L}^{-1}[\mathscr{X}(r,s)] = \frac{1}{2\pi\mathrm{i}}\int_{\gamma-\mathrm{i}\infty}^{\gamma+\mathrm{i}\infty} e^{st}\mathscr{X}(r,s)\,\mathrm{d}s, \tag{40}$$

and all the singularities are on the left-hand side of the real number γ.

From (37), it is apparent when

$$Z_n(s) = \sum_{m^*=1}^{\infty}\frac{J_1^2(\alpha_{nm^*}r_0)}{\mathscr{K}(s,\alpha_{nm^*})\,\Omega_{nm^*}} = 0, \tag{41}$$

the summation term and $\mathscr{X}(r,s)$ are singular. Equation (41) is equivalent to the expression of the natural frequencies of the tank, as presented in Eq. (39) in [20]. Therefore, $Z_n = 0$ at $s = \pm\mathrm{i}\omega_{n,m}$, where $\omega_{n,m}$ denote the natural frequencies of the tank, with subscripts n and m referring to the numbers of nodal diameters and circles, respectively. These roots lie on the imaginary axis of complex plane s and are symmetrically distributed with respect to the origin.

To check whether there are other roots in Eq. (41), we may write $s = s_R + \mathrm{i}s_I$, and substitute it into (41). We have

$$Z_n(s) = \sum_{m^*=1}^{\infty}\frac{J_n^2(\alpha_{nm^*}r_0)(A_{nm} - \mathrm{i}B_{nm})}{(A_{nm}^2 + B_{nm}^2)\Omega_{nm^*}} = 0, \tag{42}$$

where

$$A_{nm} = L\alpha_{nm^*}^4 + \rho g + (s_R^2 - s_I^2)\left(m_e + \frac{\rho}{\alpha_{nm^*}\tanh\alpha_{nm^*}H}\right), \tag{43}$$

$$B_{nm} = 2s_R s_I\left(m_e + \frac{\rho}{\alpha_{nm^*}\tanh\alpha_{nm^*}H}\right). \tag{44}$$

We may split (42) as

$$\begin{cases} \displaystyle\sum_{m^*=1}^{\infty} \frac{J_n^2(\alpha_{nm^*} r_0) A_{nm}}{(A_{nm}^2 + B_{nm}^2)\Omega_{nm^*}} = 0 \\ \displaystyle 2 s_R s_I \sum_{m^*=1}^{\infty} \frac{J_n^2(\alpha_{nm^*} r_0)\left(m_e + \dfrac{\rho}{\alpha_{nm^*}\tanh\alpha_{nm^*} H}\right)}{(A_{nm}^2 + B_{nm}^2)\Omega_{nm^*}} = 0 \end{cases}. \tag{45ab}$$

As $\alpha_{nm^*}^2 r_0^2 - n^2 > 0$ (i.e., Table 9.5 in [27]) and from Eq. (23), $\Omega_{nm^*} > 0$. This means that each term in the series in Eq. (45*b*) is positive and its left-hand side can be zero only if $s_I = 0$ or $s_R = 0$. For the former, each term in (45*a*) will be positive and the summation cannot be zero. This means that only the latter is possible or $Z_n(s) = 0$ has solutions only on the imaginary axis, or $s = \pm \mathrm{i}\omega_{n,m}$. Thus, we use the residual theorem on the left-hand side of γ. From (40), we have

$$\mathfrak{L}^{-1}[\mathscr{X}(r,s)] = \sum_{m=1}^{\infty} \mathrm{Res}\left(e^{st}\mathscr{X}(r,s), s = \pm \mathrm{i}\omega_{1,m}\right) = \sum_{m=1}^{\infty} -\rho r_0 \frac{\pm \mathrm{i}\omega_{1,m} e^{\pm \mathrm{i}\omega_{1,m} t}}{Z_1'(\pm\omega_{1,m})} \sum_{m^*=1}^{\infty} \frac{J_1(\alpha_{1m^*} r)\, J_1(\alpha_{1m^*} r_0) X_{m^*}^{(\mathscr{U})}(\pm\omega_{1,m})}{\mathscr{K}(\pm\omega_{1,m}, \alpha_{1m^*})\ \alpha_{1m^*}^2 \Omega_{1m^*}}, \tag{46}$$

where Z_n' refers to taking derivative with respect to s, $Z_n'(\pm\omega_{n,m}) = Z_n'(s = \pm \mathrm{i}\omega_{n,m})$, $\mathscr{K}(\pm\omega_{n,m}, \alpha_{nm^*}) = \mathscr{K}(s = \pm \mathrm{i}\omega_{n,m}, \alpha_{nm^*})$, $X_{m^*}^{(\mathscr{U})}(\pm\omega_{1,m}) = X_{m^*}^{(\mathscr{U})}(s = \pm \mathrm{i}\omega_{1,m})$ and $\pm$ means that both positive and negative values should be included in the summation. Using the convolution theorem, we have

$$\mathfrak{L}^{-1}[\mathscr{U}(s)\mathscr{X}(s)] = \int_0^t U(t-\tau) \sum_{m=1}^{\infty} \mathrm{Res}\left(e^{s\tau}\mathscr{X}(s), s = \pm \mathrm{i}\omega_{1,m}\right) \mathrm{d}\tau. \tag{47}$$

We may also use the convolution theorem to treat the inverse Laplace transform for the rest term in (39), as

$$\begin{aligned} &\mathfrak{L}^{-1}\left[\frac{1}{Z_n}\sum_{m^*=1}^{\infty} \frac{J_n(\alpha_{nm^*} r) X_{nm^*}^{(\mathscr{P})}}{\mathscr{K}(s, \alpha_{nm^*})\ \Omega_{nm^*}}\right] \\ &= \sum_{m^*=1}^{\infty} \mathfrak{L}^{-1}\left[\mathscr{H}_{nm^*}(s) \times \frac{1}{Z_n}\ \frac{J_n(\alpha_{nm^*} r)}{\mathscr{K}(s, \alpha_{nm^*})\ \Omega_{nm^*}} \sum_{m'=1}^{\infty} \frac{J_n^2(\alpha_{nm'} r_0)}{\Omega_{nm'}\mathscr{K}(s, \alpha_{nm'})}\right] \\ &- \sum_{m'=1}^{\infty} \mathfrak{L}^{-1}\left[\mathscr{H}_{nm'}(s) \times \frac{1}{Z_n}\ \frac{J_n(\alpha_{nm'} r_0)}{\mathscr{K}(s, \alpha_{nm'})\ \Omega_{nm'}} \sum_{m^*=1}^{\infty} \frac{J_n(\alpha_{nm^*} r) J_n(\alpha_{nm^*} r_0)}{\Omega_{nm^*}\mathscr{K}(s, \alpha_{nm^*})}\right] \\ &= \sum_{m^*=1}^{\infty} \int_0^t H_{nm^*}(t-\tau) \\ &\times \sum_{m=1}^{\infty} \mathrm{Res}\left(\frac{e^{s\tau}}{Z_n}\ \frac{J_n(\alpha_{nm^*} r)}{\mathscr{K}(s, \alpha_{nm^*})\ \Omega_{nm^*}} \sum_{m'=1}^{\infty} \frac{J_n^2(\alpha_{nm'} r_0)}{\Omega_{nm'}\mathscr{K}(s, \alpha_{nm'})}, s = \pm \mathrm{i}\omega_{n,m}\right) \mathrm{d}\tau \\ &- \sum_{m'=1}^{\infty} \int_0^t H_{nm'}(t-\tau) \\ &\times \sum_{m=1}^{\infty} \mathrm{Res}\left(\frac{e^{s\tau}}{Z_n}\ \frac{J_n(\alpha_{nm'} r_0)}{\mathscr{K}(s, \alpha_{nm'})\ \Omega_{nm'}} \sum_{m^*=1}^{\infty} \frac{J_n(\alpha_{nm^*} r) J_n(\alpha_{nm^*} r_0)}{\Omega_{nm^*}\mathscr{K}(s, \alpha_{nm^*})}, s = \pm \mathrm{i}\omega_{n,m}\right) \mathrm{d}\tau \end{aligned} \tag{48}$$

where

$$H_{nm}(t) = \int_0^{r_0} P_n(r,t)\ r\ J_n(\alpha_{nm} r)\ \mathrm{d}r. \tag{49}$$

From (39), we have

$$
\begin{aligned}
&W(r,\theta,t)\\
&=-2\mathrm{i}\rho r_0\cos\theta\times\sum_{m=1}^{\infty}\left[\frac{\omega_{1,m}}{Z_1'(\omega_{1,m})}\sum_{m^*=1}^{\infty}\frac{J_1(\alpha_{1m^*}r)J_1(\alpha_{1m^*}r_0)X_{m^*}^{(\mathscr{U})}(\omega_{1,m})}{\mathscr{K}(\omega_{1,m},\alpha_{1m^*})\ \alpha_{1m^*}^2\Omega_{1m^*}}\right]\\
&\times\int_0^t U(t-\tau)\cos\omega_{1,m}\tau\mathrm{d}\tau\\
&+\sum_{n=0}^{\infty}\cos n\theta\\
&\times\left\{\sum_{m^*=1}^{\infty}\int_0^t H_{nm^*}(t-\tau)\right.\\
&\times\sum_{m=1}^{\infty}\left(\frac{2\mathrm{i}\sin\omega_{n,m}\tau}{Z_n'(\omega_{n,m})}\ \frac{J_n(\alpha_{nm^*}r)}{\mathscr{K}(\omega_{n,m},\alpha_{nm^*})\ \Omega_{nm^*}}\sum_{m'=1}^{\infty}\frac{J_n^2(\alpha_{nm'}r_0)}{\Omega_{nm'}\mathscr{K}(\omega_{n,m},\alpha_{nm'})}\right)\mathrm{d}\tau\\
&-\sum_{m'=1}^{\infty}\int_0^t H_{nm'}(t-\tau)\\
&\left.\times\sum_{m=1}^{\infty}\left(\frac{2\mathrm{i}\sin\omega_{n,m}\tau}{Z_n'(\omega_{n,m})}\ \frac{J_n(\alpha_{nm'}r_0)}{\mathscr{K}(\omega_{n,m},\alpha_{nm'})\ \Omega_{nm'}}\sum_{m^*=1}^{\infty}\frac{J_n(\alpha_{nm^*}r)J_n(\alpha_{nm^*}r_0)}{\Omega_{nm^*}\mathscr{K}(\omega_{n,m},\alpha_{nm^*})}\right)\mathrm{d}\tau\right\},
\end{aligned}
\tag{50}
$$

where the features that $\mathscr{K}(-\omega_{n,m},\ \alpha_{n,m})=\ \mathscr{K}(\omega_{n,m},\ \alpha_{n,m})$ and $Z_n'(-\omega_{n,m})=-Z_n'(\omega_{n,m})$ have been used. In addition, an alternative form of Eq. (50) may be derived to check numerical results, which is displayed in Appendix A.

To understand the distribution of the natural frequencies better, we may inspect the roots of $Z_n(\omega)=0$ more carefully, where

$$
Z_n(\omega)=Z_n(s=\mathrm{i}\omega)=\sum_{m^*=1}^{\infty}\frac{J_n^2(\alpha_{nm^*}r_0)}{\mathscr{K}(\omega,\alpha_{nm^*})\Omega_{nm^*}}.
\tag{51}
$$

We notice that $\mathscr{K}_{n,m^*}(\omega)=\mathscr{K}(\omega,\alpha_{nm^*})=0$ has two roots and we may denote them as $\pm\varpi_{n,m^*}$ and ϖ_{n,m^*} increases with m^*. We then notice $Z_n\left(\varpi_{n,m^*}^+\right)\to-\infty$ as $\mathscr{K}_{n,m^*}\left(\varpi_{n,m^*}^+\right)\to0^-$, and $Z_n\left(\varpi_{n,m^*+1}^-\right)\to\infty$ as $\mathscr{K}_{n,m^*+1}\left(\varpi_{n,m^*+1}^-\right)\to0^+$. Thus, $Z_n(\omega)=0$ has at least one root between ϖ_{n,m^*} and ϖ_{n,m^*+1}. Also, as it is obvious from (51) that $Z_n'(\omega)>0$, $Z_n(\omega)=0$ will have only one solution within this range.

We may also consider the limit $h\to0$ in a way similar that in [28] and [29]. For the free surface flow problem, the thickness of the plate cover $h=0$, which gives $L=0$ and $m_e=0$. The natural frequency will be $\varpi_{n,m^*}^2=g\alpha_{nm^*}\tanh\alpha_{nm^*}H$ ([30,13]). Here if we take $L=0$ and $m_e=0$ directly in (31), the series becomes divergent, or $Z_n(\omega)=+\infty$. Therefore, we may consider a very small h. We expect that in such a case $Z_n(\omega)$ generally is very large and is positive. Also, based on the above discussion, we still expect that $Z_n(\omega)=0$ has a root between ϖ_{n,m^*} and ϖ_{n,m^*+1}. This is possible only if ω is sufficiently close to ϖ_{n,m^*}^+ where a large negative value of $\frac{J_n^2(\alpha_{nm^*}r_0)}{\mathscr{K}_{n,m^*}(\omega)\ \Omega_{nm^*}}$ can cancel the large positive value from the rest of the summation. We then expect $h\to0$, or $L\to0$, $m_e\to0$, $\omega\to\varpi_{n,m^*}=\sqrt{g\alpha_{nm^*}\tanh\alpha_{nm^*}H}$, which is the same as that of the free surface flow problem. We therefore can conclude that as $h\to0$, the result tends to that of the free surface flow.

The derivation procedure above is for a plate cover, but it can be readily adapted to deal with cases involving a membrane cover. In fact, we can replace $L\nabla^4\mathscr{W}(s)$ with $-T\nabla^2\mathscr{W}(s)$ in Eq. (11). Equation (20) then becomes

$$
-\frac{TI_m}{\Omega_{nm}}+\left(m_es^2+\rho g\right)e_{nm}(s)+\rho s\varphi_{nm}(s)=\frac{\mathscr{H}_{nm}}{\Omega_{nm}}-\frac{\rho s\mathscr{U}(s)\delta_{n1}}{\Omega_{nm}}\times\frac{r_0^2\ J_2(\alpha_{1m}r_0)}{\alpha_{1m}},
\tag{52}
$$

where

$$
I_m=r_0J_n(\alpha_{nm}r_0)\left.\frac{\partial\mathscr{W}_n}{\partial r}\right|_{r=r_0}-\alpha_{nm}^2e_{nm}\Omega_{nm},
\tag{53}
$$

while Eq. (21) remains the same. This gives

$$
e_{nm}(s)=\frac{\left\{\mathscr{H}_{nm}-\frac{\rho s\mathscr{U}(s)r_0^2\ J_2(\alpha_{1m}r_0)\delta_{n1}}{\alpha_{1m}}+Tr_0J_n(\alpha_{nm}r_0)\left.\frac{\partial\mathscr{W}_n}{\partial r}\right|_{r=r_0}\right\}}{\mathscr{K}_M(s,\alpha_{nm})\ \Omega_{nm}},
\tag{54}
$$

where

$$\mathscr{K}_M(s,\alpha_{nm}) = T\alpha_{nm}^2 + \rho g + s^2\left(m_e + \frac{\rho}{\alpha_{nm}\tanh\alpha_{nm}H}\right), \tag{55}$$

with subscript M referring to membrane.

Imposing edge condition $\mathscr{W}_n(r=r_0)=0$ through Eq. (19), we have

$$\left.\frac{\partial \mathscr{W}_n}{\partial r}\right|_{r=r_0} = \frac{Y_{M,n}}{Z_{M,n}}, \tag{56}$$

where

$$Y_{M,n} = Y_{M,n}^{(\mathscr{P})} + Y_{M,n}^{(\mathscr{U})} = -\frac{1}{Tr_0}\sum_{m=1}^{\infty}\frac{\mathscr{H}_{nm}(s)J_n(\alpha_{nm}r_0)}{\mathscr{K}_M(s,\alpha_{nm})\ \Omega_{nm}} + \frac{\rho s\mathscr{U}(s)\delta_{n1}}{T}\sum_{m=1}^{\infty}\frac{J_1^2(\alpha_{1m}r_0)}{\mathscr{K}_M(s,\alpha_{1m})\ \Omega_{1m}\alpha_{1m}^2} \tag{57}$$

and

$$Z_{M,n} = \sum_{m=1}^{\infty}\frac{J_n^2(\alpha_{nm}r_0)}{\mathscr{K}_M(s,\alpha_{nm})\ \Omega_{nm}}. \tag{58}$$

The final solution can then be obtained through the inverse Laplace transform, which can be written as

$$\begin{aligned}
&W(r,\theta,t)\\
&= -2\mathrm{i}\rho r_0\cos\theta \times \sum_{m=1}^{\infty}\left[\frac{\omega_{1,m}}{Z'_{M,1}(\omega_{1,m})}\sum_{m^*=1}^{\infty}\frac{J_1(\alpha_{1m^*}r)J_1(\alpha_{1m^*}r_0)X_{M,m^*}^{(\mathscr{U})}(\omega_{1,m})}{\mathscr{K}_M(\omega_{1,m},\alpha_{1m^*})\ \alpha_{1m^*}^2\Omega_{1m^*}}\right]\\
&\times\int_0^t U(t-\tau)\cos\omega_{1,m}\tau\,\mathrm{d}\tau\\
&+\sum_{n=0}^{\infty}\cos n\theta\\
&\times\left\{\sum_{m^*=1}^{\infty}\int_0^t H_{nm^*}(t-\tau)\right.\\
&\times\sum_{m=1}^{\infty}\left(\frac{2\mathrm{i}\sin\omega_{n,m}\tau}{Z'_{M,n}(\omega_{n,m})}\ \frac{J_n(\alpha_{nm^*}r)}{\mathscr{K}_M(\omega_{n,m},\alpha_{nm^*})\ \Omega_{nm^*}}\sum_{m'=1}^{\infty}\frac{J_n^2(\alpha_{nm'}r_0)}{\Omega_{nm'}\mathscr{K}_M(\omega_{n,m},\alpha_{nm'})}\right)\mathrm{d}\tau\\
&-\sum_{m'=1}^{\infty}\int_0^t H_{nm'}(t-\tau)\\
&\times\left.\sum_{m=1}^{\infty}\left(\frac{2\mathrm{i}\sin\omega_{n,m}\tau}{Z'_{M,n}(\omega_{n,m})}\ \frac{J_n(\alpha_{nm'}r_0)}{\mathscr{K}_M(\omega_{n,m},\alpha_{nm'})\ \Omega_{nm'}}\sum_{m^*=1}^{\infty}\frac{J_n(\alpha_{nm^*}r)J_n(\alpha_{nm^*}r_0)}{\Omega_{nm^*}\mathscr{K}_M(\omega_{n,m},\alpha_{nm^*})}\right)\mathrm{d}\tau\right\},
\end{aligned} \tag{59}$$

where

$$X_{M,m^*}^{(\mathscr{U})}(\omega_{1,m}) = \sum_{m'=1}^{\infty}\frac{J_1^2(\alpha_{1m'}r_0)}{\mathscr{K}_M(\omega_{1,m},\alpha_{1m'})\ \Omega_{1m'}}\left(1-\frac{\alpha_{1m^*}^2}{\alpha_{1m'}^2}\right), \tag{60}$$

with $Z_{M,n}(\omega_{n,m}) = Z_{M,n}(s=\mathrm{i}\omega_{n,m})$, $\mathscr{K}_M(\omega_{n,m},\alpha_{nm^*}) = \mathscr{K}_M(s=\mathrm{i}\omega_{n,m},\alpha_{nm^*})$ and $\omega_{n,m}$ are the natural frequencies of the tank, which are the roots of the equation $Z_{M,n}(\omega)=0$.

The velocity potential can be also obtained. From (15) and (21), we have

$$\mathscr{F}(r,\theta,z,s) = \mathscr{U}(s)\ r\cos\theta + \sum_{n=0}^{\infty}\cos n\theta\sum_{m=1}^{\infty}\frac{J_n(\alpha_{nm}r)\ se_{nm}(s)}{\alpha_{nm}\sinh\alpha_{nm}H}\cosh\alpha_{nm}(z+H), \tag{61}$$

throughout the fluid domain. Next, we perform the inverse Laplace transform to (61) directly to get $\Phi(r,\theta,z,t)$ for the plate cover case as

$$\begin{aligned}
&\Phi(r,\theta,z,t) = \mathfrak{L}^{-1}[\mathscr{F}(r,\theta,z,s)]\\
&= r\cos\theta\mathfrak{L}^{-1}[\mathscr{U}(s)] + \sum_{n=0}^{\infty}\cos n\theta\sum_{m^*=1}^{\infty}\frac{J_n(\alpha_{nm^*}r)\cosh\alpha_{nm^*}(z+H)}{\alpha_{nm^*}\sinh\alpha_{nm^*}H}\mathfrak{L}^{-1}[se_{nm^*}(s)].
\end{aligned} \tag{62}$$

Here we may work out the inverse Laplace transform to $se_{nm}(s)$ by directly using the kinematic condition (3), (50) and (62), and comparing the coefficients of $J_1(\alpha_{1m}r)$ on both sides, which yields

$$\begin{aligned}
&\mathfrak{L}^{-1}[se_{nm^*}(s)]\\
&= -2\mathrm{i}\rho r_0\delta_{n1}\times\sum_{m=1}^{\infty}\left[\frac{\omega_{1,m}}{Z_1(\omega_{1,m})}\frac{J_1(\alpha_{1m^*}r_0)X_{m^*}^{(\mathscr{H})}(\omega_{1,m})}{\mathscr{K}(\omega_{1,m},\alpha_{1m^*})\ \alpha_{1m^*}^2\Omega_{1m^*}}\right]\frac{\mathrm{d}F_m}{\mathrm{d}t}\\
&+\sum_{m=1}^{\infty}\left(\frac{2\mathrm{i}}{Z_n'(\omega_{n,m})}\ \frac{1}{\mathscr{K}(\omega_{n,m},\alpha_{nm^*})\ \Omega_{nm^*}}\sum_{m'=1}^{\infty}\frac{J_n^2(\alpha_{nm'}r_0)}{\Omega_{nm'}\mathscr{K}(\omega_{n,m},\alpha_{nm'})}\right)\\
&\times\frac{\mathrm{d}}{\mathrm{d}t}\int_0^t H_{nm^*}(t-\tau)\sin\omega_{n,m}\tau\mathrm{d}\tau\\
&-\sum_{m'=1}^{\infty}\sum_{m=1}^{\infty}\left(\frac{2\mathrm{i}}{Z_n'(\omega_{n,m})}\ \frac{J_n(\alpha_{nm'}r_0)}{\mathscr{K}(\omega_{n,m},\alpha_{nm'})\ \Omega_{nm'}}\ \frac{J_n(\alpha_{nm^*}r_0)}{\Omega_{nm^*}\mathscr{K}(\omega_{n,m},\alpha_{nm^*})}\right)\\
&\times\frac{\mathrm{d}}{\mathrm{d}t}\int_0^t H_{nm'}(t-\tau)\ \sin\omega_{n,m}\tau\mathrm{d}\tau,
\end{aligned}\tag{63}$$

where $F_m = \int_0^t U(t-\tau)\cos\omega_{1,m}\tau\mathrm{d}\tau$.

3. Energy analysis

Energy of the coupled system is also of interest to investigate. The total energy, denoted as E_{total}, of this sloshing system contains four parts, which can be written as

$$E_{total} = K_l + K_e + T_l + T_e, \tag{64}$$

where K and T refer to the potential and kinetic energies respectively, and subscripts l and e refer to the fluid and elastic cover respectively. T_l can be written as [1]

$$T_l = -\frac{\rho}{2}\oiint_S\Phi\Phi_n\mathrm{d}S = \frac{\rho}{2}\int_0^{2\pi}\int_0^{r_0}\Phi|_{z=0}\Phi_z|_{z=0}r\mathrm{d}\theta\mathrm{d}r + \frac{\rho}{2}\int_0^{2\pi}\int_{-H}^{0}\Phi|_{r=r_0}\Phi_r|_{r=r_0}r_0\mathrm{d}\theta\mathrm{d}z, \tag{65}$$

where S denotes the entire boundary surface of fluid domain and Φ_n denotes the inward normal derivative. In addition, as the deflection of the fluid is the same with that of the cover, the potential energy of the liquid can be therefore expressed as

$$K_l = \frac{\rho g}{2}\int_0^{2\pi}\int_0^{r_0}W^2(r,\theta,t)r\mathrm{d}\theta\mathrm{d}r. \tag{66}$$

The kinetic energy of the cover is

$$T_e = \frac{m_e}{2}\int_0^{2\pi}\int_0^{r_0}\left(\frac{\partial W}{\partial t}\right)^2 r\mathrm{d}\theta\mathrm{d}r. \tag{67}$$

The potential energy of the cover consists of two parts: one from the variation of vertical deflection, similar to that of the wave elevation, and the other from bending strain energy. Therefore, we may write it as

$$K_e = K_e^{(1)} + K_e^{(2)}, \tag{68}$$

where

$$K_e^{(1)} = \frac{m_e g}{2}\int_0^{2\pi}\int_0^{r_0}W^2(r,\theta,t)r\mathrm{d}\theta\mathrm{d}r, \tag{69}$$

and

$$K_e^{(2)} = \iint_S \frac{L}{2}\left\{\left(\frac{\partial^2 W}{\partial x^2}+\frac{\partial^2 W}{\partial y^2}\right)^2 - 2(1-\nu)\left[\frac{\partial^2 W}{\partial x^2}\frac{\partial^2 W}{\partial y^2} - \left(\frac{\partial^2 W}{\partial x \partial y}\right)^2\right]\right\}\mathrm{d}x\mathrm{d}y$$
$$= \frac{L}{2}\iint_S \left\{(\nabla^2 W)^2 - 2(1-\nu)\left[\frac{W_{rr}W_r}{r}+\frac{W_{rr}W_{\theta\theta}}{r^2} - \left(\frac{W_\theta}{r^2}-\frac{1}{r}W_{r\theta}\right)^2\right]\right\} r\mathrm{d}r\mathrm{d}\theta. \tag{70}$$

For the tank with motion $U(t)$, K_l can be obtained by substituting the first term of (50) into (66), as

$$K_l = -2\pi\rho^3 r_0^2 g \sum_{m^*=1}^{\infty} J_1^2(\alpha_{1m^*}r_0) - \alpha_{1m^*}^4 \Omega_{1m^*} \mathfrak{T}_{m^*}^2, \tag{71}$$

where

$$\mathfrak{T}_{m^*} = \sum_{m=1}^{\infty} \frac{\omega_{1,m}F_m(t)}{Z_1(\omega_{1,m})} \frac{X_{m^*}^{(\mathscr{H})}(\omega_{1,m})}{\mathscr{H}(\omega_{1,m},\alpha_{1m^*})}, \tag{72}$$

while T_l can be similarly obtained from (65) as

$$T_l = \frac{\rho\pi r_0^2 H U^2(t)}{2} - 2\mathrm{i}\pi\rho^2 r_0^2 U(t) \sum_{m^*=1}^{\infty} \frac{J_1^2(\alpha_{1m^*}r_0)}{\alpha_{1m^*}^4 \Omega_{1m^*}} \frac{\mathrm{d}\mathfrak{T}_{m^*}}{\mathrm{d}t} - 2\pi\rho^3 r_0^2 \sum_{m^*=1}^{\infty} \frac{J_1^2(\alpha_{1m^*}r_0)}{\alpha_{1m^*}^5 \Omega_{1m^*} \tanh\alpha_{1m^*}H} \left(\frac{\mathrm{d}\mathfrak{T}_{m^*}}{\mathrm{d}t}\right)^2. \tag{73}$$

In addition, from (67) and (69), we have

$$T_e = \frac{m_e}{2}\int_0^{2\pi}\int_0^{r_0}\left(\frac{\partial W}{\partial t}\right)^2 r\mathrm{d}\theta\mathrm{d}r = -2\rho^2 r_0^2 m_e \pi \sum_{m^*=1}^{\infty} \frac{J_1^2(\alpha_{1m^*}r_0)}{\alpha_{1m^*}^4 \Omega_{1m^*}} \left(\frac{\mathrm{d}\mathfrak{T}_{m^*}}{\mathrm{d}t}\right)^2, \tag{74}$$

and

$$K_e^{(1)} = \frac{m_e g}{2}\int_0^{2\pi}\int_0^{r_0} W^2(r,\theta,t) r\mathrm{d}\theta\mathrm{d}r = \frac{m_e K_l}{\rho}. \tag{75}$$

For $K_e^{(2)}$, we consider the second integral in $K_e^{(2)}$, by using Green's theorem, we have

$$I_2 = \iint_S \left[\frac{\partial^2 W}{\partial x^2}\frac{\partial^2 W}{\partial y^2} - \left(\frac{\partial^2 W}{\partial x\partial y}\right)^2\right]\mathrm{d}x\mathrm{d}y = \iint_S \left[\frac{\partial}{\partial x}\left(\frac{\partial W}{\partial x}\frac{\partial^2 W}{\partial y^2}\right) - \frac{\partial}{\partial y}\left(\frac{\partial W}{\partial x}\frac{\partial^2 W}{\partial x\partial y}\right)\right]\mathrm{d}x\mathrm{d}y = \oint_C \left[\left(\frac{\partial W}{\partial x}\frac{\partial^2 W}{\partial y^2}\right)n_x - \left(\frac{\partial W}{\partial x}\frac{\partial^2 W}{\partial x\partial y}\right)n_y\right]\mathrm{d}s. \tag{76}$$

Specifically, for a circle with radius of r_0, (76) can be transformed to the polar coordinate system as

$$I_2 = \int_0^{2\pi}\left[\frac{\sin 2\theta}{2r}W_r W_{r\theta} + \frac{\cos^2\theta}{r}W_r^2 + \frac{\cos^2\theta}{r^2}W_r W_{\theta\theta} - \frac{\sin 2\theta}{r^2}W_\theta W_r - \frac{\sin^2\theta}{r^2}W_\theta W_{r\theta} - \frac{\sin 2\theta}{2r^3}W_\theta W_{\theta\theta} + \frac{\sin^2\theta}{r^3}W_\theta^2\right]_{r=r_0}$$
$$r_0\mathrm{d}\theta = \int_0^{2\pi}\left[-\frac{\sin 2\theta}{2r^3}W_\theta W_{\theta\theta} + \frac{\sin^2\theta}{r^3}W_\theta^2\right]_{r=r_0} r_0\mathrm{d}\theta = -2\pi\rho^2\left[\sum_{m^*=1}^{\infty}\frac{J_1^2(\alpha_{1m^*}r_0)}{\alpha_{1m^*}^2\Omega_{1m^*}}\mathfrak{T}_{m^*}\right]^2, \tag{77}$$

where the edge condition has been used.

For the first integral, we have

$$I_1 = \iint_S (\nabla^2 W)^2 \mathrm{d}S = \iint_S \nabla(\nabla W\,\nabla^2 W - W\nabla^3 W)\mathrm{d}S + \iint_S W\nabla^4 W r\mathrm{d}S = \int_0^{2\pi}\left(\frac{\partial W}{\partial n}\nabla^2 W - W\frac{\partial \nabla^2 W}{\partial n}\right)\mathrm{d}s + \iint_S W\nabla^4 W r\mathrm{d}S. \tag{78}$$

Specifically, for clamped edge case, the first term of (78) reduces to zero. Using the dynamic equation, or (2*a*), to replace $\nabla^4 W$, we have

$$I_1 = \iint_S W\nabla^4 W r\mathrm{d}S = -\frac{\rho g}{L}\iint_S W^2 r\mathrm{d}\theta\mathrm{d}r - \frac{\rho}{L}\iint_S W\Phi_t r\mathrm{d}\theta\mathrm{d}r - \frac{m_e}{L}\iint_S W W_{tt} r\mathrm{d}\theta\mathrm{d}r$$
$$= -\frac{2K_l}{L} + \frac{2\pi\mathrm{i}\rho^2 r_0^3}{L}\frac{\mathrm{d}U}{\mathrm{d}t}\sum_{m^*=1}^{\infty}\frac{J_1(\alpha_{1m^*}r_0)J_2(\alpha_{1m^*}r_0)}{\alpha_{1m^*}^3\Omega_{1m^*}}\mathfrak{T}_{m^*} + \frac{4\pi\rho^2 r_0^2}{L}\sum_{m^*=1}^{\infty}\frac{J_1^2(\alpha_{1m^*}r_0)}{\alpha_{1m^*}^4\Omega_{1m^*}}\mathfrak{T}_{m^*}\frac{\mathrm{d}^2\mathfrak{T}_{m^*}}{\mathrm{d}t^2}\left(\frac{\rho}{\alpha_{1m^*}\tanh\alpha_{1m^*}H} + m_e\right). \tag{79}$$

4. Results and analysis

Based on the linear assumption, the excitation due to tank motion $U(t)$ and external pressure $P(r,\theta,t)$ can be considered separately.

4.1. Excitation due to tank motion

The effect of a given $U(t)$ is considered in this section, and the resultant deflection of the flexible plate and membrane cover can be respectively obtained from the first term of Eqs. (50) and (59). Here, we may let $U(t) = \sin\omega_0 t$ as an example, and therefore

$$F_m = \int_0^t \sin\omega_0(t-\tau)\cos\omega_{1,m}\tau \mathrm{d}\tau = \frac{\omega_0\left(\cos\omega_{1,m}t - \cos\omega_0 t\right)}{\omega_0^2 - \omega_{1,m}^2}. \tag{80}$$

In general, Eq. (80) shows that under sinusoidal excitation with frequency ω, the motion will have a sinusoidal component at the same frequency. In addition to that, the motion will have the sinusoidal modes at the natural frequencies. When the excitation frequency approaches to one of the natural frequencies, or $\omega_0 \to \omega_{1,m}$, (80) will approach

$$\lim_{\omega_0\to\omega_{1,m}} F_m = \lim_{\omega_0\to\omega_{1,m}} \frac{\omega_0\left(\cos\omega_{1,m}t - \cos\omega_0 t\right)}{\omega_0^2 - \omega_{1,m}^2} = \frac{t}{2}\sin\omega_{1,m}t. \tag{81}$$

This means that the motion will tend to infinity as time increases, which is a common feature at resonance without damping.

In the following calculation, we utilise dimensionless parameters based on the acceleration due to gravity g, the radius of the circular cylindrical tank r_0, and the density of liquid ρ. The Poisson's ratio is set to 0.3. For the case study, we may select parameters with $H^* = H/r_0 = 1$, $m_e^* = m_e/(\rho r_0) = 5 \times 10^{-4}$ and $L^* = L/\left(\rho g r_0^4\right) = 1 \times 10^{-3}$, as in [20]. From Eq. (50), it can be seen as m increases the term decays at a rate of $1/m^4$ as the leading of α_{1m} is proportional of m (Eq. 9.5.13 of [27]). We obtain the first ten natural frequencies $\omega_{1,m}$ ($m = 1,2,\ldots 10$) from Eq. (41), which are displayed in Table 1 for the clamped edge case. To obtain the defection, the series in the first term of Eq. (50) regarding m^* is truncated at $M^* = 10$, as terms beyond that is of order 10^{-4}. Numerical results from larger M^* are found to make no visual difference, as expected from the above asymptotic analysis.

We may choose three locations on the elastic cover along the radial direction of the tank, aligned with the direction of oscillation (in the first term of Eq. (50), $\cos\theta$ can be taken out as a factor), namely, $(r,\theta) = (0.25,0)$, $(0.50,0)$ and $(0.75,0)$, to display the time series results of cover deflection in Fig. 2. Eight excitation frequencies are chosen, namely, $\omega_0 = 1.0,\ 1.8,\ 1.9,\ 1.9512\ (\omega_{1,1}),\ 2.0,\ 2.1, 4.0$ and $5.1672(\omega_{1,2})$. The first ten natural modes have been included and inclusion of additional natural modes will not alter the results visibly. At the same excitation frequency, the time-series curves of different locations show similar oscillatory features due to same harmonic elements they have, but with different amplitudes.

In the first term of Eq. (50), the mth term in the summation contains two harmonic oscillations at $\omega_{1,m}$ and ω_0, respectively. At a given ω_0, the magnitude of the mth term decays at a rate of $1/\omega_{1,m}^2$. Thus, unless $\omega_{1,m}$ is close to ω_0, its contribution is small when m is large. In general, when ω_0 is away from all the natural frequencies $\omega_{1,m}$ ($m = 1,2,3\ldots$), the variation of W with t has many frequency components, and the curves may look like irregular, as can be seen from Fig. 2(a). When ω_0 is near one of the natural frequencies, say $\omega_0 \approx \omega_{1,1}$, the first term in the first series of (50) will become far more significant than the others, the reason of which can be clearly seen from (80). The term has two components: (i). $\omega_{1,m}$ or ω_0 (as they are very close) and (ii). the envelope wave with frequency $|\omega_{1,1} - \omega_0|/2$. This can be clearly seen in Fig. 2(b) and becomes even more evident in Fig. 2(c). When $\omega_0 = \omega_{1,1}$, there is only one component at ω_0 but the amplitude keeps increasing with time, the reason of which can be seen from Eq. (81). When ω_0 is close to one of the other natural frequencies, similar behaviour can be expected. In addition, Fig. 2(h) shows the result at $\omega_0 = \omega_{1,2}$, which is similar to that in Fig. 2(d). It is worth mentioning that in the case of an ideal fluid, resonance leads to unbounded oscillation amplitudes due to the absence of dissipative forces. In such a case, the effect of the fluid viscosity is important, due to which the motion will not tend to infinity. Also, nonlinearity may become important when the motion amplitude is large.

The time histories of the kinetic energy and potential energy of elastic cover and liquid are respectively plotted in Fig.s 3 and 4 against different ω_0. From the graphs, we can observe that all energy components oscillate cyclically over time, demonstrating repeated energy transfers among these four energy components within the system. Regarding the peak magnitudes, $T_l > K_l > K_e \gg T_e$ is consistently observed across all study cases. This illustrates that the liquid is the primary energy carrier in the system, with its kinetic energy dominating the overall system dynamics, while the elastic cover stores energy through its deformation. When the tank is undergoing forced motion, the energy from external forcing is first transformed into the liquid. The elastic cover plays an important role in constraining the liquid motion and absorbs part of the energy in the forms of its own potential and kinetic energy. When resonance occurs, we can see though all the energy components oscillate over time, but their peaks keep growing with time, as the

Table 1
Natural frequencies $\omega_{n,m}$ at $L^* = 1 \times 10^{-3}$, $m_e^* = 5 \times 10^{-4}$ and $H^* = 1$ for clamped edge.

	$m=1$	$m=2$	$m=3$	$m=4$	$m=5$	$m=6$	$m=7$	$m=8$	$m=9$	$m=10$
$n=1$	1.95119	5.16721	11.5683	21.8401	36.4541	55.8465	80.422	110.557	146.604	188.893
$n=2$	3.08284	7.69070	15.9067	28.2407	45.1437	67.0351	94.304	127.315	166.406	211.901

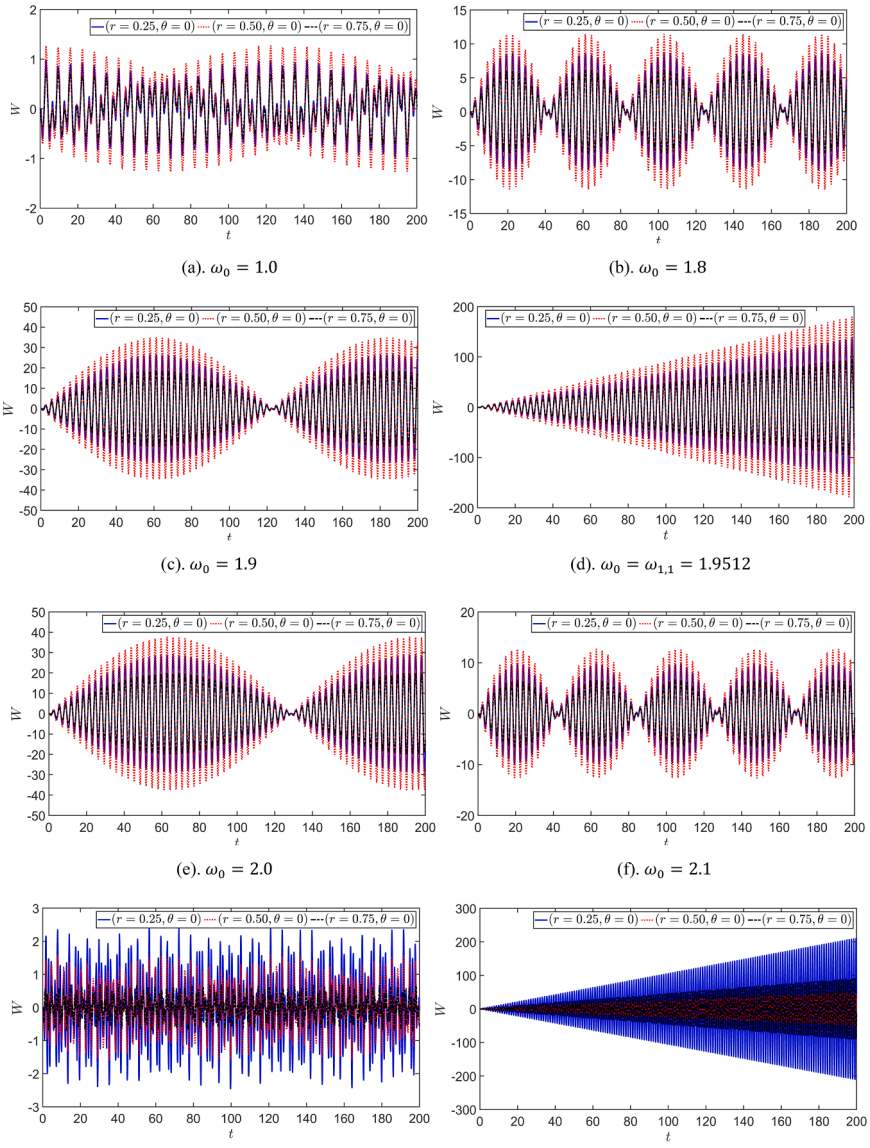

(a). $\omega_0 = 1.0$ (b). $\omega_0 = 1.8$

(c). $\omega_0 = 1.9$ (d). $\omega_0 = \omega_{1,1} = 1.9512$

(e). $\omega_0 = 2.0$ (f). $\omega_0 = 2.1$

(g). $\omega_0 = 4$ (h). $\omega_0 = \omega_{1,2} = 5.1672$

Fig. 2. . Time series of plate deflections at three locations $(r,\theta) = (0.25,\ 0)$, $(0.50, 0)$ and $(0.75,\ 0)$ for the clamped edge case at different excitation frequencies. ($L^* = 1 \times 10^{-3}$, $m_e^* = 5 \times 10^{-4}$ and $H^* = 1$).

entire system continuously obtains energy from external forces.

4.2. Motion due to external pressure excitation on the cover

Next, we consider the motion due to the external pressure. In (14), we may further define $P_n(r,t)$ as

$$P_n(r,t) = \cos\omega_0 t \sum_{m'=1}^{\infty} p_{nm'} J_n(\alpha_{nm'} r). \tag{82}$$

From (49) and (82), we have

$$H_{nm}(t) = p_{nm}\Omega_{nm} \cos\omega_0 t, \tag{83}$$

and the second term of (50), defined as W_{ep}, becomes

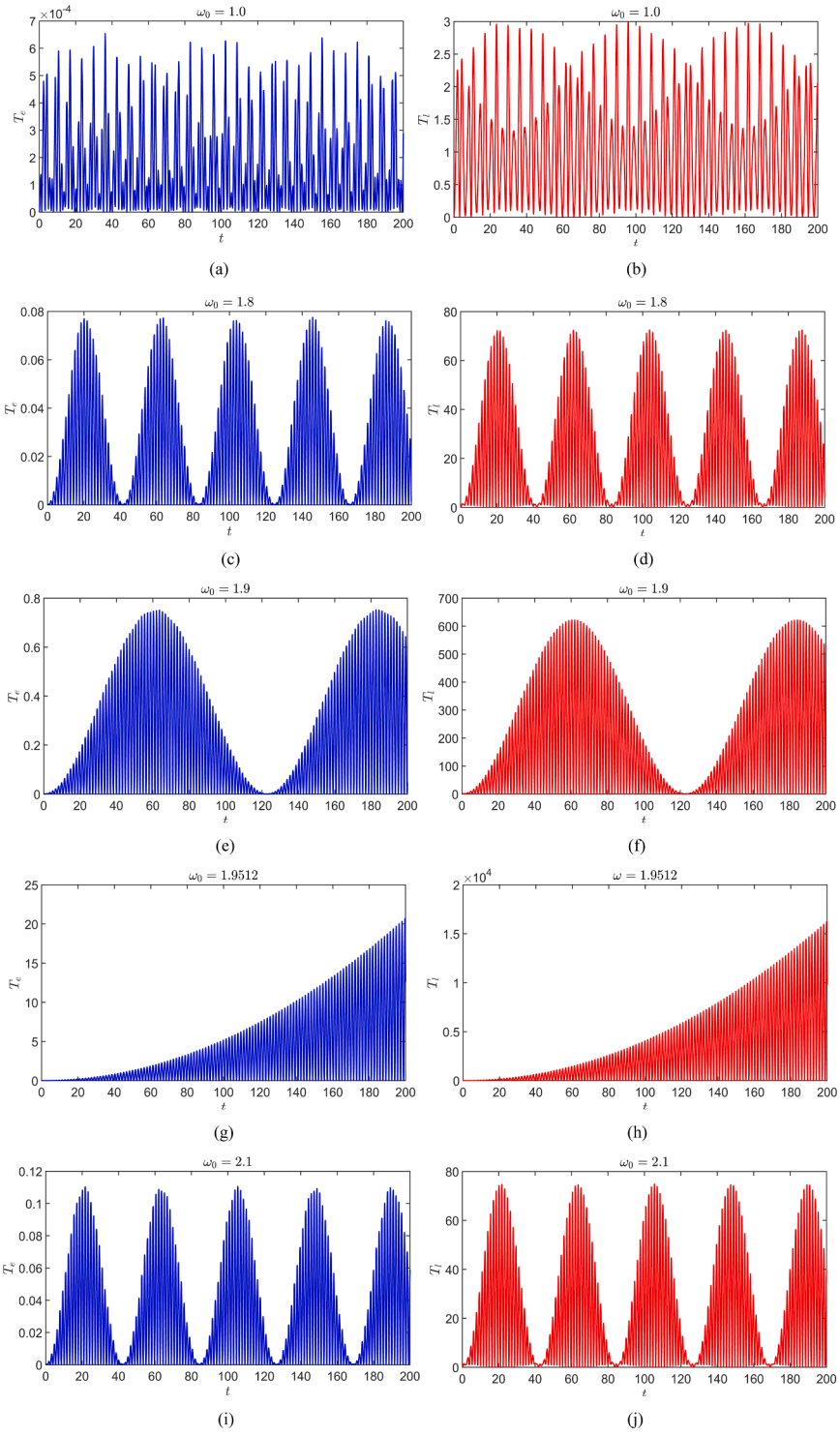

Fig. 3. Time histories of kinetic energy of the elastic plate cover and liquid at different frequencies.

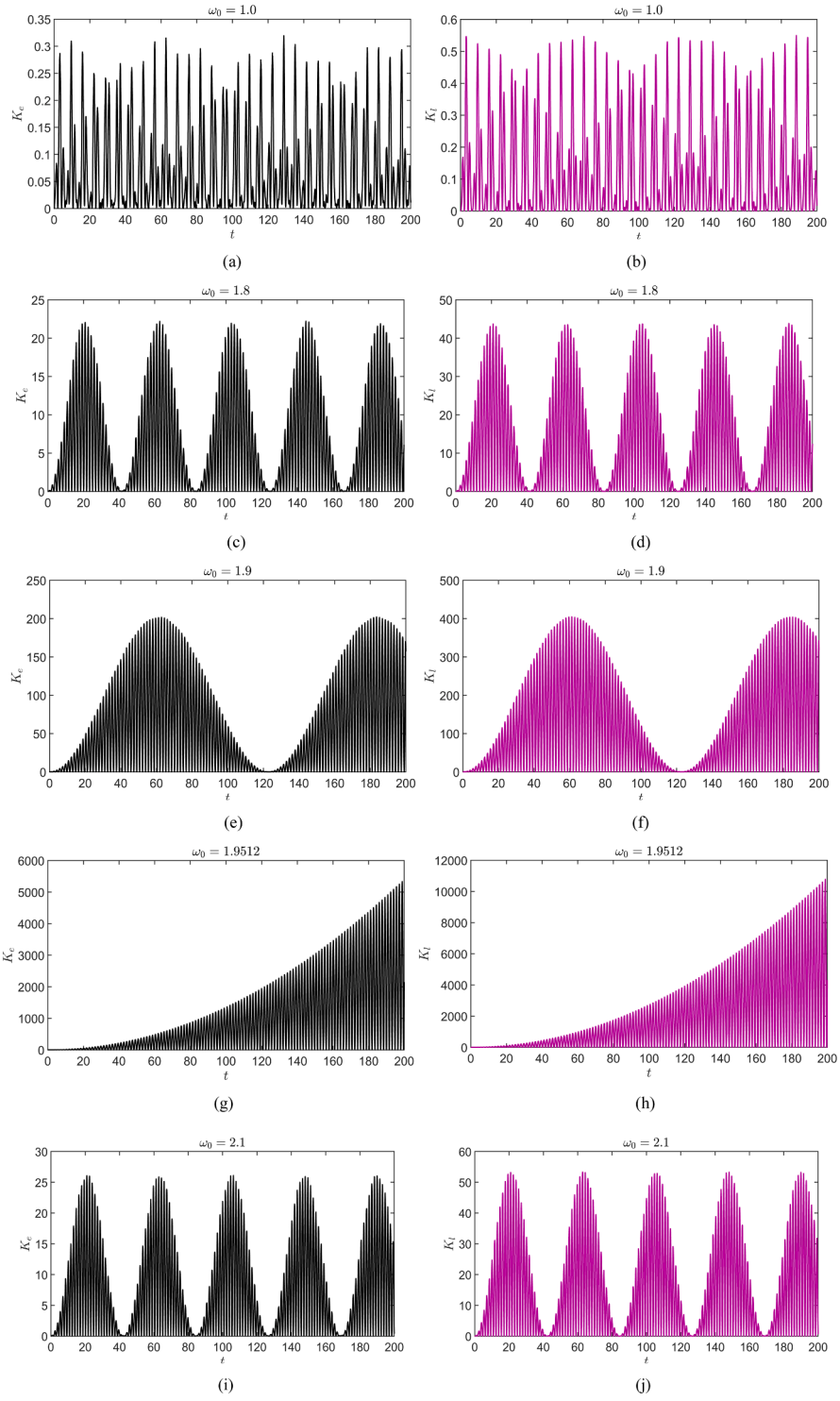

Fig. 4. Time histories of potential energy of the elastic plate cover and liquid at different frequencies.

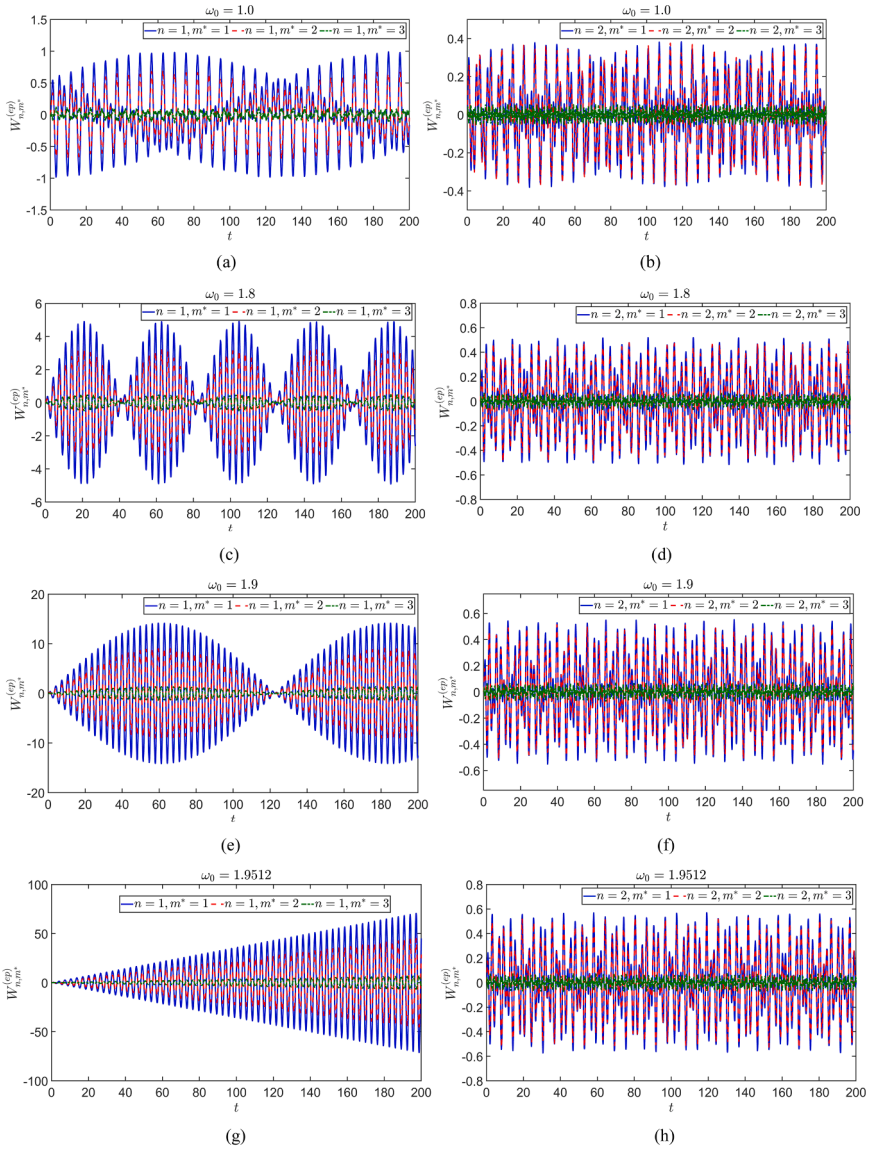

Fig. 5. Time series of $W^{(ep)}_{n,m^*}$ at the location of $(r, \theta) = (0.50, 0)$ for the clamped edge case at different excitation frequencies. ($L^* = 1 \times 10^{-3}$, $m_e^* = 5 \times 10^{-4}$ and $H^* = 1$).

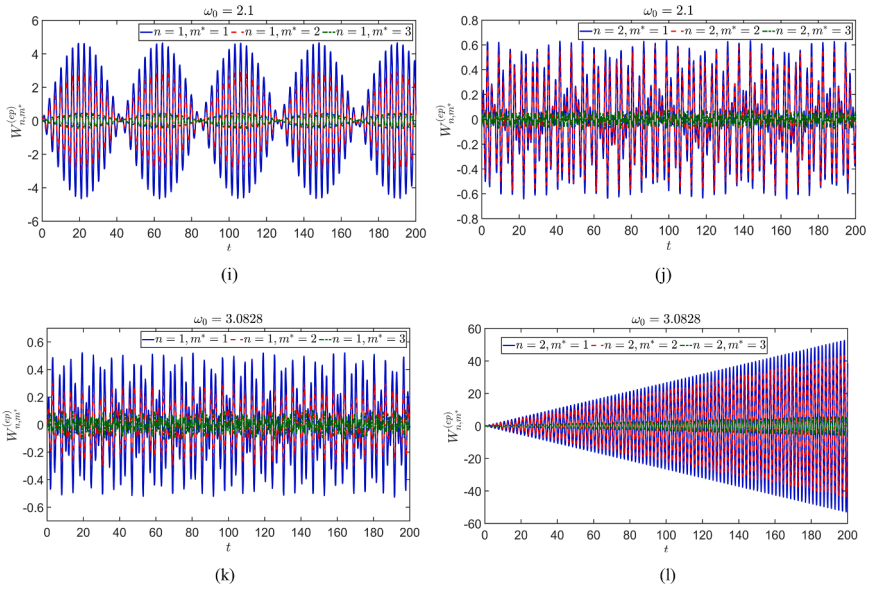

Fig. 5. (*continued*).

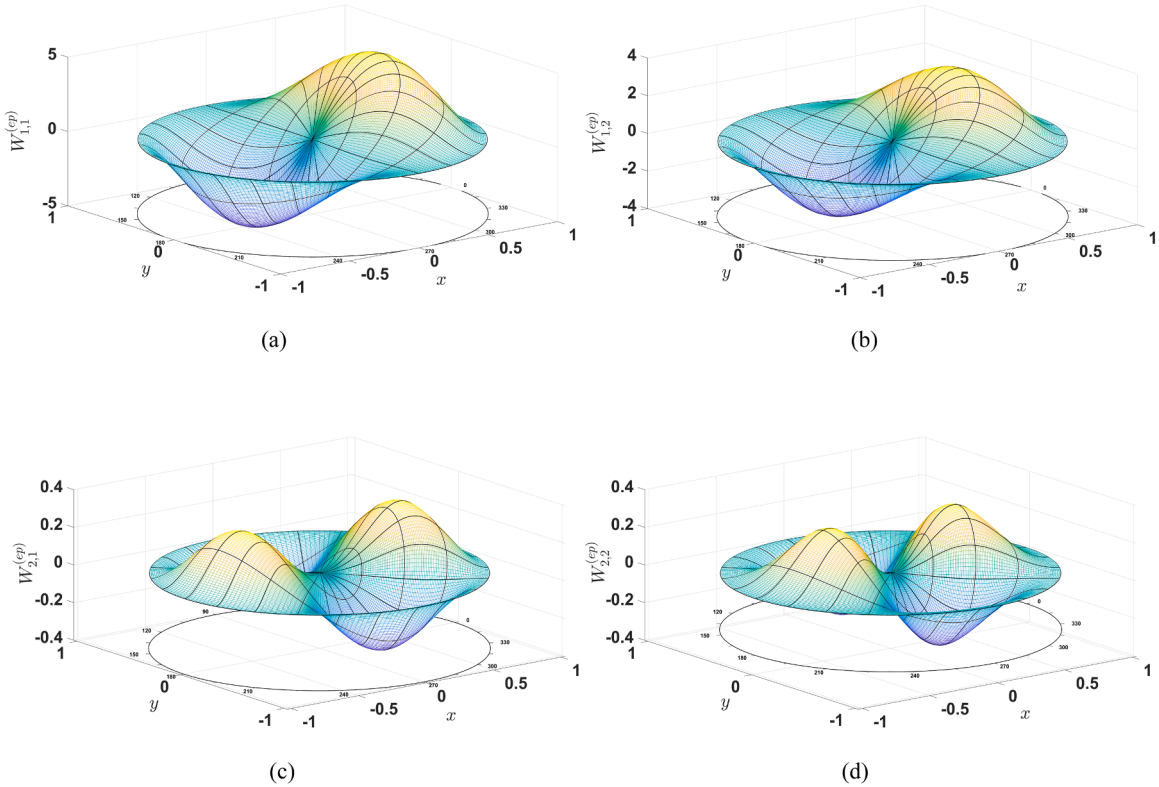

Fig. 6. Surface plot of the resultant plate deflection $W^{(ep)}_{n,m^*}$.

$$
\begin{aligned}
W_{ep} &= \sum_{n=0}^{\infty} \cos n\theta \Bigg\{ \sum_{m^*=1}^{\infty} p_{nm^*} J_n(\alpha_{nm^*} r) \sum_{m=1}^{\infty} \left(\frac{2\mathrm{i} G_{n,m}(t)}{Z_n'(\omega_{n,m}) \mathscr{K}(\omega_{n,m}, \alpha_{nm^*})} \sum_{m'=1}^{\infty} \frac{J_n^2(\alpha_{nm'} r_0)}{\Omega_{nm'} \mathscr{K}(\omega_{n,m}, \alpha_{nm'})} \right) \\
&\quad - \sum_{m'=1}^{\infty} p_{nm'} J_n(\alpha_{nm'} r_0) \sum_{m=1}^{\infty} \left(\frac{2\mathrm{i} G_{n,m}(t)}{Z_n'(\omega_{n,m}) \mathscr{K}(\omega_{n,m}, \alpha_{nm'})} \sum_{m^*=1}^{\infty} \frac{J_n(\alpha_{nm^*} r) J_n(\alpha_{nm^*} r_0)}{\Omega_{nm^*} \mathscr{K}(\omega_{n,m}, \alpha_{nm^*})} \right) \Bigg\} \\
&= \sum_{n=0}^{\infty} \cos n\theta \Bigg\{ \sum_{m^*=1}^{\infty} p_{nm^*} \sum_{m=1}^{\infty} \left(\frac{2\mathrm{i} G_{n,m}(t)}{Z_n'(\omega_{n,m}) \mathscr{K}(\omega_{n,m}, \alpha_{nm^*})} \right. \\
&\quad \left. \times \sum_{m'=1}^{\infty} \frac{J_n(\alpha_{nm'} r_0) [J_n(\alpha_{nm'} r_0) J_n(\alpha_{nm^*} r) - J_n(\alpha_{nm'} r) J_n(\alpha_{nm^*} r_0)]}{\Omega_{nm'} \mathscr{K}(\omega_{n,m}, \alpha_{nm'})} \right) \Bigg\},
\end{aligned}
\tag{84}
$$

where

$$
G_{n,m}(t) = \int_0^t \sin\omega_{n,m}\tau \cos\omega_0(t-\tau) \mathrm{d}\tau = \begin{cases} \dfrac{\omega_{n,m} \left(\cos\omega_{n,m} t - \cos\omega_0 t\right)}{\omega_0^2 - \omega_{n,m}^2}, & \omega_0 \neq \omega_{n,m} \\ \dfrac{t}{2} \sin\omega_{n,m} t, & \omega_0 \to \omega_{n,m} \end{cases}. \tag{85}
$$

Because of linearity, the term related to each p_{nm^*} can be considered separately, or

$$
W_{nm^*}(r,\theta) = \cos n\theta \sum_{m=1}^{\infty} \left(\frac{2\mathrm{i} G_{n,m}(t)}{Z_n'(\omega_{n,m}) \mathscr{K}(\omega_{n,m}, \alpha_{nm^*})} \times \sum_{m'=1}^{\infty} \frac{J_n(\alpha_{nm'} r_0) [J_n(\alpha_{nm'} r_0) J_n(\alpha_{nm^*} r) - J_n(\alpha_{nm'} r) J_n(\alpha_{nm^*} r_0)]}{\Omega_{nm'} \mathscr{K}(\omega_{n,m}, \alpha_{nm'})} \right). \tag{86}
$$

For the results due to an arbitrary external pressure, they can be obtained by superposition. Similar to Fig. 2, we display the resultant deflections $W_{n,m^*}^{(ep)}$ at the position $(r,\theta) = (0.50,\ 0)$ for cases of different excitation frequencies in Fig. 5. For $n = 1$, the amplitudes of the curves corresponding to $m^* = 1$ are significantly larger than these for $m^* = 2$, as observed in the graphs on the left-hand side of the figure. For $n = 2$, the amplitudes of the curves for $m^* = 1$ become comparable to those for $m^* = 2$. When the external frequencies approach ω_{n,m^*}, the envelope becomes apparent in the curves of $W_{n,m^*}^{(ep)}$. In addition, resonance occurs at $\omega_0 = \omega_{n,m^*}$, with the amplitudes of the curves for $W_{n,m^*}^{(ep)}$ continuously increasing.

In addition, surface plots are also provided to show the entire plate deflection at certain time instants. In Fig. 6, the graphs for $W_{n,m^*}^{(ep)}$ $(n,m^* = 1,2)$ at $\omega_0 = 1.8$ at $t = 20.94$ are displayed. The variation of these graphs along the circumferential direction and its rotational symmetry depends on the term $\cos n\theta$, where n refers to the number of the nodal diameters. We can expect that with the increase of n, there will be more oscillations in the circumferential direction.

5. Conclusions

The transient liquid motion coupled with an elastic membrane or plate cover, in a cylindrical container, under forced horizontal motion and external pressure applied to the elastic cover, is investigated. An analytical solution scheme is developed based on the Laplace transform and the Bessel-Fourier series expansion, allowing the calculation of the time-varying variables in the coupled vibration system. Explicit solutions for the deflection of elastic cover and energy components in the system have been derived. An alternative form of expression based on the residual theorem has also been provided for verification.

When the tank undergoes forced motion, the frequency components of the time history of the upper surface deflection are determined by the excitation frequency and the natural frequencies of the system. This can lead to three different scenarios: the presence of multiple frequency components, two dominant components, or a single frequency component at resonance. In addition, the cyclical oscillation of energy components within the vibrating system highlights the dynamic energy transfer among them. Energy from external forces is primarily transferred into the liquid, with the elastic cover constraining the motion of the liquid and storing part of the energy mainly through deformation. The liquid serves as the primary energy carrier. At resonance, the energy peaks continuously grow.

With external pressure on the cover, the motion response of the upper surface can be analysed for each component, enabling the study of any arbitrary pressure distributions. The circumferential variation and rotational symmetry depend on the term $\cos n\theta$, with higher nodal diameters leading to increased angular oscillations.

CRediT authorship contribution statement

K. Ren: Writing – review & editing, Writing – original draft, Methodology, Investigation, Formal analysis, Conceptualization. **G.X. Wu:** Writing – review & editing, Writing – original draft, Methodology, Investigation, Formal analysis, Conceptualization.

Declaration of competing interest

The authors declare that they have no known competing financial interests or personal relationships that could have appeared to influence the work reported in this paper.

Acknowledgement

This work is supported by the Royal Society Research Grants (RG\R1\251348).

Appendix A. Alternative forms of the summations in Eq. (50)

For the summation with respect to m^*, or

$$S_1 = \sum_{m^*=1}^{\infty} \frac{J_1(\alpha_{1m^*}r)J_1(\alpha_{1m^*}r_0)X_{m^*}^{(\mathscr{K})}(\omega_{1,m})}{\mathscr{K}(\omega_{1,m},\alpha_{1m^*})\ \alpha_{1m^*}^2\Omega_{1m^*}} \tag{A0}$$

in (50), we define a complex function below

$$f_1(\alpha) = \frac{2J_1(\alpha r)X(\omega,\alpha)}{r_0\mathscr{K}(\omega,\alpha)\ J_1(\alpha r_0)\alpha^2}, \tag{A1}$$

where

$$X(\omega,\alpha) = \sum_{m=1}^{\infty} \frac{J_1^2(\alpha_{1m}r_0)}{\mathscr{K}(\omega,\alpha_{1m})\ \Omega_{1m}}\left(1-\frac{\alpha^2}{\alpha_{1m}^2}\right). \tag{A2}$$

We can integrate $f_1(\alpha)$ along a circle of infinite radius R centred at the origin in the complex plane α and use residue theorem at $\mathscr{K}(\omega,k_{m'})=0$ and $J_1(\alpha_{1m^*}r_0)=0$. The roots of $\mathscr{K}(\omega,k_{m'})=0$ involve four fully complex roots denoted as $\pm k_{-2}$, $\pm k_{-1}$, two real roots denoted as $\pm k_0$, and infinite pure imaginary roots denoted as $\pm k_{m'}$ ($m'=1,2,3\ldots$), e.g., [20]. Therefore, we have

$$I_1 = \frac{1}{2\pi i}\oint_c f_1(\alpha)\mathrm{d}\alpha = 2\left(\sum_{m'=-2}^{\infty}\frac{2J_1(k_{m'}r)X(\omega,k_{m'})}{r_0\mathscr{K}'(\omega,k_{m'})\ J_1'(k_{m'}r_0)k_{m'}^2} + \sum_{m^*=1}^{\infty}\frac{2J_1(\alpha_{1m^*}r)X(\omega,\alpha_{1m^*})}{r_0^2\mathscr{K}(\omega,\alpha_{1m^*})\ J_1''(\alpha_{1m^*}r_0)\alpha_{1m^*}^2}\right) = 0. \tag{A3}$$

Here,

$$\mathscr{K}'(\omega,k_{m'}) = \frac{\partial\mathscr{K}(\omega,\alpha=k_{m'})}{\partial\alpha} = \frac{2\rho\omega^2 S_{m'}}{k_{m'}\tanh^2 k_{m'}H}, \tag{A4}$$

where

$$S_{m'} = \frac{2Lk_{m'}^4\tanh^2 k_{m'}H}{\rho\omega^2} + \frac{\sinh 2k_{m'}H + 2Hk_{m'}}{4k_{m'}\cosh^2 k_{m'}H}, \tag{A5}$$

as defined in Eq. (45) in [20].

With (A3), and also notice that $\Omega_{nm^*} = -r_0^2 J_n''(\alpha_{nm^*}r_0)J_n(\alpha_{nm^*}r_0)/2$ after the recurrence relations (Eq. 9.1.27, [27]) and $J_n'(\alpha_{nm^*}r_0)=0$ are used, we have

$$\sum_{m^*=1}^{\infty}\frac{J_1(\alpha_{1m^*}r)J_1(\alpha_{1m^*}r_0)X_{m^*}^{(\mathscr{K})}(\omega_{1,m})}{\mathscr{K}(\omega_{1,m},\alpha_{1m^*})\ \alpha_{1m^*}^2\Omega_{1m^*}} = -\sum_{m^*=1}^{\infty}\frac{2\ J_1(\alpha_{1m^*}r)\ X(\omega_{1,m},\alpha_{1m^*})}{r_0^2\mathscr{K}(\omega_{1,m},\alpha_{1m^*})\ \alpha_{1m^*}^2\ J_1''(\alpha_{1m^*}r_0)} = \sum_{m'=-2}^{\infty}\frac{2J_1(k_{m'}r)X(\omega_{1,m},k_{m'})}{r_0\mathscr{K}'(\omega_{1,m},k_{m'})\ J_1'(k_{m'}r_0)k_{m'}^2}. \tag{A6}$$

For $Z_n'(\omega_{n,m})$ in (50), from (51), we have

$$Z_n'(\omega) = -\sum_{m^*=1}^{\infty}\frac{J_n^2(\alpha_{nm^*}r_0)}{\mathscr{K}^2(\omega,\alpha_{nm^*})\Omega_{nm^*}}\frac{\mathrm{d}\mathscr{K}(\omega,\alpha_{nm^*})}{\mathrm{d}\omega} = \sum_{m^*=1}^{\infty}\frac{2J_n(\alpha_{nm^*}r_0)}{r_0^2\mathscr{K}^2(\omega,\alpha_{nm^*})J_n''(\alpha_{nm^*}r_0)}\frac{\mathrm{d}\mathscr{K}(\omega,\alpha_{nm^*})}{\mathrm{d}\omega}. \tag{A7}$$

We may apply the residue theorem first to transform $Z(\omega)$. To do this, we may define a complex function as

$$f_2(\alpha) = \frac{2J_n(\alpha r_0)}{r_0\mathscr{K}(\omega,\alpha)\ J_n'(\alpha r_0)}. \tag{A8}$$

Then,

$$I_2 = \frac{1}{2\pi i}\oint_c f_2(\alpha)\mathrm{d}\alpha = 2\left(\sum_{m'=-2}^{\infty}\frac{2J_n(k_{m'}r_0)}{r_0\mathscr{K}'(\omega,k_{m'})\ J_n'(k_{m'}r_0)} + \sum_{m^*=1}^{\infty}\frac{2J_n(\alpha_{nm^*}r_0)}{r_0^2\mathscr{K}(\omega,\alpha_{nm^*})\ J_n''(\alpha_{nm^*}r_0)}\right) = 0. \tag{A9}$$

This gives

$$Z(\omega)=\sum_{m^*=1}^{\infty}\frac{J_n^2(\alpha_{nm^*}r_0)}{\mathscr{K}(\omega,\alpha_{nm^*})\ \Omega_{nm^*}}=-\sum_{m^*=1}^{\infty}\frac{2J_n(\alpha_{nm^*}r_0)}{\mathscr{K}(\omega,\alpha_{nm^*})\ r_0^2J_n''(\alpha_{nm^*}r_0)}=\sum_{m'=-2}^{\infty}\frac{2J_n(k_{m'}r_0)}{r_0\mathscr{K}'(\omega,\ k_{m'})\ J_n'(k_{m'}r_0)}, \tag{A10}$$

where $\mathscr{K}'$ means derivative with respect to α, as displayed in (A4). We then have

$$\begin{aligned}Z'&=\frac{\mathrm{d}Z}{\mathrm{d}\omega}=\frac{\mathrm{d}}{\mathrm{d}\omega}\sum_{m'=-2}^{\infty}\frac{2J_n(k_{m'}r_0)}{r_0\mathscr{K}'(\omega,\ k_{m'})\ J_n'(k_{m'}r_0)}=\frac{2}{r_0}\sum_{m'=-2}^{\infty}\frac{\mathrm{d}}{\mathrm{d}\omega}\left\{\frac{J_n(k_{m'}r_0)}{\mathscr{K}'(\omega,\ k_{m'})\ J_n'(k_{m'}r_0)}\right\}\\&=\frac{2}{r_0}\sum_{m'=-2}^{\infty}\frac{\left\{\begin{array}{c}r_0J_n'(k_{m'}r_0)\dfrac{\mathrm{d}k_{m'}}{\mathrm{d}\omega}\times\mathscr{K}'\ J_n'(k_{m'}r_0)\\-J_n(k_{m'}r_0)\left[\dfrac{\mathrm{d}\mathscr{K}'}{\mathrm{d}\omega}J_n'(k_{m'}r_0)+\mathscr{K}'\ r_0J_n''(k_{m'}r_0)\dfrac{\mathrm{d}k_{m'}}{\mathrm{d}\omega}\right]\end{array}\right\}}{\left[\mathscr{K}'\ J_n'(k_{m'}r_0)\right]^2}.\end{aligned} \tag{A11}$$

We notice that $k_{m'}$ is a solution of $\mathscr{K}(\omega,\alpha)=0$ and is therefore function of ω. From $\mathrm{d}\mathscr{K}=0$ we have

$$\frac{\mathrm{d}k_{m'}}{\mathrm{d}\omega}=-\frac{\left(\frac{\partial\mathscr{K}}{\partial\omega}\right)}{\left(\frac{\partial\mathscr{K}}{\partial k_{m'}}\right)}=\frac{\left(Lk_{m'}^4+\rho g\right)k_{m'}\tanh^2k_{m'}H}{\rho\omega^3S_{m'}}. \tag{A12}$$

In (A11), $\mathrm{d}\mathscr{K}'/\mathrm{d}\omega$ can be obtained by applying $\mathrm{d}/\mathrm{d}\omega$ to (A4), as

$$\Gamma_{m'}=\frac{\mathrm{d}\mathscr{K}'}{\mathrm{d}\omega}=\frac{\partial\mathscr{K}'}{\partial\omega}+\frac{\partial\mathscr{K}'}{\partial k_{m'}}\frac{\mathrm{d}k_{m'}}{\mathrm{d}\omega}=\frac{4\rho\omega S_{m'}}{k_{m'}\tanh^2k_{m'}H}-\frac{12Lk_{m'}^3}{\omega}-\frac{4\rho g}{\omega k_{m'}}+\frac{4\left(Lk_{m'}^4+\rho g\right)\left(5Lk_{m'}^3\tanh^2k_{m'}H-\frac{\rho\omega^2H^2}{\sinh2k_{m'}H}\right)}{\rho\omega^3S_{m'}}. \tag{A13}$$

Therefore, (A11) can be further written as

$$Z'\left(\omega=\omega_{1,m}\right)=\frac{1}{r_0}\sum_{m'=-2}^{\infty}\frac{k_{m'}^2\tanh^4k_{m'}H}{2\rho^2\omega^4S_{m'}^2}\times\left[\frac{2r_0\left(Lk_{m'}^4+\rho g\right)}{\omega}\left(1-\frac{J_n(k_{m'}r_0)J_n''(k_{m'}r_0)}{\left(J_n'(k_{m'}r_0)\right)^2}\right)-\frac{\Gamma_{m'}J_n(k_{m'}r_0)}{J_n'(k_{m'}r_0)}\right]. \tag{A14}$$

Data availability

Data will be made available on request.

References

[1] H. Lamb, Hydrodynamics, Cambridge University Press, Cambridge, UK, 1932.
[2] B. Budiansky, Sloshing of liquids in circular canals and spherical tanks, J. Aerosp. Sci. 27 (1960) 161–173, https://doi.org/10.2514/8.8467.
[3] H.N. Abramson, W.H. Chu, L.R. Garza, Liquid sloshing in spherical tanks, AIAA J. 1 (2) (1963) 384–389, https://doi.org/10.2514/3.1542.
[4] P. McIver, Sloshing frequencies for cylindrical and spherical containers filled to an arbitrary depth, J. Fluid Mech. 201 (1989) 243–257, https://doi.org/10.1017/S0022112089000923.
[5] G.X. Wu, R.Eatock Taylor, D.M. Greaves, The effect of viscosity on the transient free-surface waves in a two-dimensional tank, J. Eng. Math. 40 (2001) 77–90, https://doi.org/10.1023/A:1017558826258.
[6] O.M. Faltinsen, A numerical nonlinear method of sloshing in tanks with two-dimensional flow, J. Sh. Res. 22 (1978) 193–202, https://doi.org/10.5957/jsr.1978.22.3.193.
[7] G.X. Wu, R.Eatock Taylor, Finite element analysis of two-dimensional non-linear transient water waves, Appl. Ocean Res. 16 (6) (1994) 363–372, https://doi.org/10.1016/0141-1187(94)00029-8.
[8] G.X. Wu, Q.W. Ma, R.Eatock Taylor, Numerical simulation of sloshing waves in a 3D tank based on a finite element method, Appl. Ocean Res. 20 (6) (1998) 337–355, https://doi.org/10.1016/S0141-1187(98)00030-3.
[9] J.B. Frandsen, Sloshing motions in excited tanks, J. Comput. Phys. 196 (1) (2004) 53–87, https://doi.org/10.1016/j.jcp.2003.10.031.
[10] B.F. Chen, R. Nokes, Time-independent finite difference analysis of fully non-linear and viscous fluid sloshing in a rectangular tank, J. Comput. Phys. 209 (1) (2005) 47–81, https://doi.org/10.1016/j.jcp.2005.03.006.
[11] D. Liu, P. Lin, A numerical study of three-dimensional liquid sloshing in tanks, J. Comput. phys. 227 (8) (2008) 3921–3939, https://doi.org/10.1016/j.jcp.2007.12.006.
[12] R.A. Ibrahim, Liquid Sloshing Dynamics: Theory And Applications, Cambridge University Press, 2005.
[13] O.M. Faltinsen, A.N. Timokha, Sloshing, Cambridge university press, Cambridge, 2009.
[14] H.F. Bauer, Frequencies of a hydroelastic rectangular system, Forsch. Ingenieurwes. 59 (1) (1993) 18–28, https://doi.org/10.1007/BF02560620.
[15] H.F. Bauer, W. Eidel, Hydroelastic vibrations in a two-dimensional rectangular container filled with frictionless liquid and a partly elastically covered free surface, J. fluids struct. 19 (2) (2004) 209–220, https://doi.org/10.1016/j.jfluidstructs.2003.11.002.
[16] H.F. Bauer, J. Siekmann, Note on linear hydroelastic sloshing, Z Angew. Math. Mech. 49 (1969) 577–589, https://doi.org/10.1002/zamm.19690491002.
[17] H.F. Bauer, Coupled frequencies of a liquid in a circular cylindrical container with elastic liquid surface cover, J. Sound Vib. 180 (5) (1995) 689–704, https://doi.org/10.1006/jsvi.1995.0109.

[18] M. Amabili, Vibrations of circular plates resting on a sloshing liquid: solution of the fully coupled problem, J. Sound Vib. 245 (2) (2001) 261–283, https://doi.org/10.1006/jsvi.2000.3560.
[19] Y.W. Kim, Y.S. Lee, Coupled vibration analysis of liquid-filled rigid cylindrical storage tank with an annular plate cover, J. Sound Vib. 279 (1-2) (2005) 217–235, https://doi.org/10.1016/j.jsv.2003.10.032.
[20] K. Ren, G.X. Wu, Z.F. Li, Natural modes of liquid sloshing in a cylindrical container with an elastic cover, J. Sound Vib. 512 (2021) 116390, https://doi.org/10.1016/j.jsv.2021.116390.
[21] R. Shen, J. Lyu, S. Wang, Coupled vibration analysis of fluid-filled baffled tank equipped with Kirchhoff plate, J. Sound Vib. 520 (2022) 116604, https://doi.org/10.1016/j.jsv.2021.116604.
[22] S.M. Kim, M.K. Kwak, Coupled vibration and sloshing analysis of the circular plate resting on the free surface of a fluid-filled cylindrical tank, J. Sound Vib. 536 (2022) 117131, https://doi.org/10.1016/j.jsv.2022.117131.
[23] H.F. Bauer, Hydroelastic vibrations in a rectangular container, Int. J. Solids Struct. 17 (7) (1981) 639–652, https://doi.org/10.1016/0020-7683(81)90001-9.
[24] K. Ren, G.X. Wu, Y.F. Yang, Coupled free vibrations of liquid in a three-dimensional rectangular container with an elastic cover, Phys. Fluids 34 (6) (2022), https://doi.org/10.1063/5.0097194.
[25] S. Timoshenko, S. Woinowsky-Krieger, Theory of plates and shells, McGraw-hill, New York, 1959.
[26] K. Ren, G.X. Wu, Z.F. Li, Hydroelastic waves propagating in an ice-covered channel, J. Fluid Mech. 886 (A8) (2020), https://doi.org/10.1017/jfm.2019.1042.
[27] M. Abramowitz, I.A. Stegun, Handbook of mathematical functions with formulas, graphs, and mathematical tables, Natl. Bur. Stand. Appl. Math. Ser. 55 (1972). Tenth Printing.
[28] Y.F. Yang, G.X. Wu, K. Ren, Hydroelastic wave interaction with a circular crack of an ice-cover in a channel, J. Fluids Struct. 130 (2024), https://doi.org/10.1016/j.jfluidstructs.2024.104173.
[29] S.Y. Sun, G.X. Wu, Sloshing in a tank with elastic side walls and a membrane cover, Phys. Fluids 36 (10) (2024), https://doi.org/10.1063/5.0238210.
[30] J.L. MacCarty, D.G. Stephens, Investigation of the natural frequencies of fluids in spherical and cylindrical tanks, National Aeronautics and Space Administration, 1960.